Validation of the SAFER HBM in Rear-Facing Upright and Reclined Position in High-Speed Frontal Impacts

Jonas Östh, Emil Gröndahl, Yun-Seok Kang, Lotta Jakobsson

Abstract Most Human Body Model (HBM) validation studies have focused on either forward-facing frontal or side impact load cases. In this study, a Finite Element (FE) model of a test setup previously used for rear-facing Post Mortem Human Subjects (PMHS) in high-speed frontal impact tests was developed and used for validation of the SAFER HBM v10 and v11 in both upright and reclined positions. First, tests performed with THOR-50M ATD in the same test setup as used for the PMHS tests were simulated to enable development and verification of the test setup FE model without tuning it with respect to the HBM results, strengthening the confidence in the subsequent HBM validation. Both evaluated SAFER HBM models compared reasonably with respect to the PMHS test data, with average ISO Scores above 0.74 for the X accelerations and displacements. The SAFER HBM v11 showed improved biofidelity with respect to Z-displacements than v10, something which has been highlighted in previous work as challenging to capture both for the THOR-50M ATD in physical testing and the GHBMC M50-O in simulations in the upright position. The potential of HBMs for evaluation of novel seating positions was demonstrated for rear-facing occupants in high-speed frontal impacts and in reclined seating positions.

Keywords Human Body Model, Finite Element, Validation, Rear-facing, Reclined

I. INTRODUCTION

Several Finite Element (FE) Human Body Models (HBMs) for vehicle crash simulations have been developed. There are two major occupant HBM families that are widely available: the Global Human Body Model Consortium (GHBMC) 5th female, 50th male and 95th percentile male detailed occupant models [1–3] and simplified occupant models [4]; and the THUMS v4 5th female, 50th male and 95th percentile models [5]. In addition to these models, the 50th male SAFER HBM [6] is being continuously developed [6,7], and recently a new version (v) 11 with an updated spine model was introduced [8].

One of the benefits of using HBMs for occupant safety analysis and development is that HBMs can be developed to be omni-directional and use local measures such as tissue strain for injury prediction. As such, they are suitable for analysis of novel vehicle concepts proposed for future vehicles, for instance reclined or rear-facing and campfire seating configurations [9–11]. However, for reliable simulation results it is important to validate HBMs in conditions similar to their application, to reduce the amount of extrapolation that is included in the analysis.

A majority of whole-body validations of HBMs for occupant simulation have focused on upright forward-facing frontal [12–15] and side impact [1, 13, 16–17] kinematic and injury prediction outcomes. These studies were enabled by the availability of Post-Mortem Human Subject (PMHS) test data to validate the HBM response. Some validations have also included novel seating, such as reclined seating positions in forward-facing frontal impact [18, 19].

For occupant rear impact responses, most PMHS tests that can be used for whole-body validation have been carried out at low [20, 21] or medium severity [22, 23]. For instance, these studies have been used for whole-body rear impact validation of the VIVA [14] and VIVA+ [24] and the GHBMC [25] HBMs. Up until recently, there has been limited availability of whole-body, high-speed, rear impact tests for HBM validation. However, one

J. Östh, PhD, (e-mail: jonas.osth@volvocars.com, tel: +46 728 88 91 72), is a Technical Expert for Human Body Modelling, E. Gröndahl is a Safety Analysis CAE Engineer and L. Jakobsson, PhD, is a Senior Technical Leader at the Volvo Cars Safety Centre, Gothenburg, Sweden. Y.-S. Kang is an Associate Professor at Ohio State University, USA. J. Östh is an Adjunct Associate Professor and L. Jakobsson an Adjunct Professor at Chalmers University of Technology, Sweden., and are both are associated with SAFER – Vehicle and Traffic Safety Centre at Chalmers in Sweden.

such study was recently conducted by [26], using a reinforced seat with an integrated seat belt in both upright and reclined seated positions, with three PMHS in each test condition. For this study, an average 56 km/h frontal impact pulse was used but the tested subjects were travelling rear-facing on a sled with a reinforced seat, generating high-speed occupant rear impact with a frontal impact pulse. Occupant kinematics and injuries were evaluated. Fractures to the upper and lower extremities as well as rib cage and pelvis were reported, and concluded to be resulting from the excessive ramping kinematics exhibited by the PMHSs.

The high-speed, rear-facing frontal impact PMHS test setup [26] was used to validate the biofidelity of the THOR-50M Anthropomorphic Test Device (ATD) [27], which was found to have more biofidelic kinematics in the reclined seated position than in the upright position. A limitation of the THOR ATD was that it did not show the same amount of spine straightening that was present in the PMHSs. Moreover, the high-speed rear-facing upright PMHS test setup [26] was modelled using the FE method also and used to validate the GHBMC M50-O v6.0 model [28]. An FE model of the seat used for the testing, from the second row of a model year 2018 Honda Odyssey and the sled interface was developed and validated with respect to tests with the Hybrid III ATD in the same condition as the PMHS tests [28]. The boundary conditions for the FE seat model were the seat back load cells that were constrained to the rigid sled, while the head restraint was modelled with a flexible constraint to reproduce the dynamic deflection of the head restraint in the tests. The validation of the GHBMC model [28] showed that the head, thoracic spine and pelvis resultant accelerations and angular Y-rotations were similar to the PMHSs, while Z-displacements were underestimated by the HBM.

The aim of the present study was to develop and verify an FE model of the sled setup used for the high-speed rear-facing frontal impact PMHS tests, in both upright and reclined seating positions, and use this FE model to validate the high-speed rear-facing frontal impact response of the SAFER HBM.

II. METHODS

An FE model of the sled and the reinforced seat with integrated seat belt system used in the high-speed, rear-facing frontal impact PMHS test [26] was first created and verified with respect to THOR test [27] responses, and then used for HBM validation with respect to the PMHS data [26] in a subsequent step. Two HBM models, the SAFER HBM v10.0 [6][7] and v11.0.1 [8], were included in the validation simulations, in both an upright and a reclined position.

Sled FE Model Development

An FE model of the seat with an integrated belt system [29] was downloaded from the National Highway Traffic Safety Administration (NHTSA) crash simulation vehicle model repository [30]. The seat model was converted to the mm-kg-ms unit system and rotated to fit the laboratory coordinate system (Z-downward, X-forward and Y to the right), Fig. 1. The seat bolster and cushion were extended further back to eliminate voids in the foam, and cushion springs were brought into contact with the cushion. The seat cushion and bolster were remeshed with 15 mm tetrahedral elements using the undeformed surface shapes from scan data of the seat [30]. A flat 2 mm plastic hard back was added to the seat, as well as a seat belt retractor structure based on publicly available spare part drawings for the model year 2018 Honda Odyssey seat. The retractor was modelled as a rigid cylinder, 46 mm wide and with a diameter of 33 mm, with a mass of 0.95 kg with a 2 mm thick plastic cover, Fig. 1. Furthermore, the weight of the whole seat assembly was adjusted to 31.2 kg as measured in the PMHS study [26], of which the seat back weighed 8.7 kg. The seat foam material was exchanged for a material based on data from [31]. This step was necessary to alleviate numerical instability during the high-speed impact. In addition, an insert with stiffer material represented by Expanded Polypropylene (EPP) [32] to increase the load in the mid-seat back was added, Fig. 1. A summary of seat and sled materials used is provided in Table AI in Appendix A. Segment based contacts (SOFT = 2) with friction coefficients of 0.3 for the belt to HBM and 0.5 for the seat to HBM were used.

The seat belt was modelled using a combination of 1-Dimensional (1D) and 2-Dimensional (2D) seat belt elements. At each end, at a rigid part above the left shoulder, and on the anchor attachment, elements which pre-tensioned the seat belt with 27 N for the shoulder belt and 18 N for the lap belt for the first 20 ms of each simulation were modelled. For the buckle, 1D seat belts and a slipring with a friction coefficient of 0.15 was used.

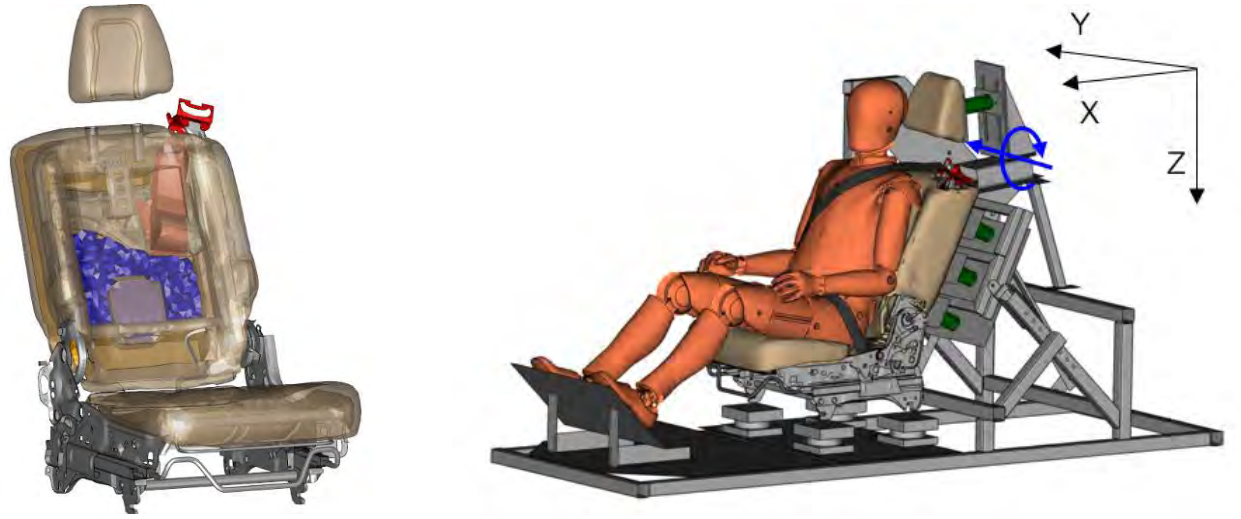

Fig. 1. Left: Updated seat with integrated belt system FE model. Indicated in red is the added retractor and plastic cover, and in blue Expanded Polypropylene (EPP) insert that was added to the model. Right: The seat model in the upright position with 25° seat back angle on the sled, with the FE THOR-50M v1.7 in position. The green cylinders behind the seat represent the load cells recording the boundary conditions in the simulations. The blue arrows show the location of the revolute joint to provide similar head restraint motion as in the physical tests.

The sled, Fig. 1, was modelled from CAD data of the sled [30] using full-integrated quadrilateral elements with characteristic lengths of 10 mm and a high-strength (Dual Phase (DP) 800) steel material model, Table AI in Appendix A. Two versions of the sled were created, one for the upright, Fig. 1, and one for the reclined positions, Fig. A1 in Appendix A. Connections were modelled using Constrained Nodal Rigid Bodies (CNRB:s) and the position of the head restraint and foot rest was parameterised to allow for adjustments to each evaluated occupant model. At the bottom of the vertical plate holding the head restraint, Fig. 1., a revolute joint with a rotational stiffness of 10,000 Nm/rad was added to replicate the motion of the head restraint recorded in the physical tests, see Fig. B2 in Appendix B. Seat back and head restraint load cells were modelled using full-integrated solid elements with a mild steel material with lowered density to match the load cell masses.

Sled FE Model Verification

For verification of the sled setup FE simulation model, the THOR-50M FE model (USNCAP version 1.7, Humanetics, Farmington Hills, MI, USA) was positioned in the seat in accordance with the protocol used for testing [27], Table AII in Appendix A. For both positions, Fig. 1 and Fig. A1 in Appendix A, the pelvis angle was prescribed to the average from the tests and the spine was extended to a lower thoracic pitch angle of −9° (erect position). For the upright position, the neck was flexed to level the head at 0° angle.

Human Body Models

The SAFER HBM v10 [6][7] and v11 [8] are 50th percentile male (M50) occupant models with a stature of 1.75 m and a mass of 77 kg. SAFER HBM v10 consists of 305,00 nodes connected by 220,000 solid elements, 191,000 shell elements and some 2,500 one-dimensional elements. It has a detailed rib cage [33], population average pelvis [34], the head is the KTH head and brain model [36] and, for instance, it has been validated for rib fracture risk and whole-body kinematics in frontal impact [35] and far-side kinematics [6].

The updated SAFER HBM v11 consists of 498,400 nodes, 382,000 solid elements, 232,000 shell elements and 3,500 one-dimensional elements. The detailed rib cage, pelvis and KTH head and brain are the same as for v10. Additional updates compared with v10 are new shoulder girdles (humeri, claviculae, scapulae), femora, ligamentous spine from L5 to C1 modelled with the methods described by [37] and [38], and updated abdominal and pelvis soft tissues.

The HBMs were positioned in the seat with the H-point 20 mm further down and back compared with the THOR FE model. For the upright position, the initial HBM position was used, with some adjustments to the arms which were positioned at the sides of the model, Fig. 2. For the reclined position, the HBMs were rotated 10° around the Y-axis in the H-point and the spine extended an additional 10° and the neck by 6° to reach a 27° Frankfort plane angle as in the tests [26], and the extremities adjusted to reach the foot rest and rest on the side

of the thighs. The head restraint position was adjusted to match the 85 mm backset and 105 mm topset used in the upright position, and 0 mm backset and 105 mm topset used in the reclined position [26]. The resulting body segment angles compared with the PMHSs can be found in Table AIII in Appendix A.

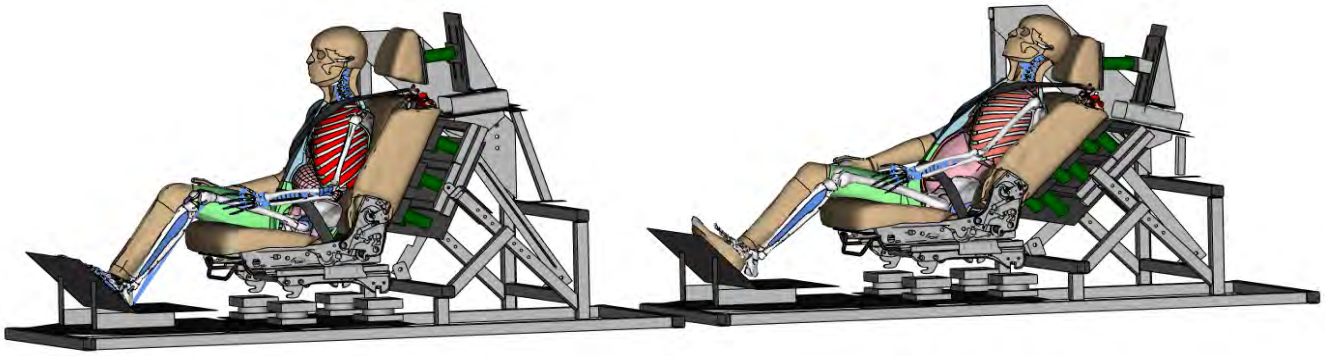

Fig. 2. Left: SAFER HBM v10 in upright position with 25° seat back angle. Right: SAFER HBM v11 in reclined position with 45° seat back angle.

Analysis

The data from the physical tests with THOR [27] was digitized from the publication for each test, while for the PMHS response corridors and average signals after processing (normalisation to the 50th male [26]) was acquired in digital format. The simulation results were compared to the average curve for each condition – the average of the three THOR tests or the corridor average for the PMHS test, using the ISO/TS 18571 method [39]. The total score was divided into one for the boundary conditions (eight signals) and one for the occupant kinematics (21 signals for THOR and 27 signals for the HBMs), Table CI in Appendix C. The ISO scores were calculated for the time interval of 0–120 ms for each simulation using the CORAplus software (v4.0.5, PDB, Gaimersheim, Germany). In addition, the upright simulations with SAFER HBM v10 and v11 were compared relative to the PMHS data using the Biofidelity Ranking System (BRS) [27, 28]. The BRS score should represent the deviation of the model from the PMHS data measured in a number of Standard Deviations (SD) which is why a lower score is better. A model response below 2 SD can be considered as Good [27]. The ISO Score evaluation results in a value in the range 0–1 and higher values are better. According to ISO/TS 18571 [39] a score ≤ 0.58 is to be considered Poor, 0.58< Fair ≥0.8, 0.8< Good ≥0.94 and >0.94 Excellent.

Accelerometer nodes were added to the HBMs at the head centre of gravity, on the anterior body of T1, T4, T8, T12 and to the iliac wings for the pelvis (the average signal of the iliac wing nodes was used) similar to the instrumentation in the PMHS testing [26]. Simulation data was recorded at 10 kHz (0.1 ms time interval) and test data was up-sampled before the ISO/TS 18571 comparison. The load cell forces were filtered with a Channel Filter Class (CFC) 60 filter [40] and inertia compensated using the load cell plate and head restraint masses (3.86 kg and 1.81 kg, respectively) multiplied with CFC60 filtered acceleration recorded in the simulation. THOR simulation data was filtered using a CFC1000 filter for accelerations and CFC60 for rotations and rotational velocities. For SAFER HBM v10 and v11 all acceleration signals were filtered using CFC60 as the HBM acceleration outputs had a much higher noise content than the FE THOR data.

Chest band deformation was calculated by tracking two nodes on the HBMs' skin, one on the ventral and one on the dorsal side, in the sagittal plane, halfway between the sternal notch and xiphoid process. The resultant change in distance normalised with the half initial chest width was compared with the PMHS data.

Explicit FE analysis was done using LS-DYNA MPP R9.3.1 (SVN 141945, ANSYS/LST, Livermore, CA), meshing in ANSA v22.1.4 (BETA CAE Systems, Luzern, Switzerland), occupant positioning using PRIMER v19.1 (OASYS Ltd., Sollihull, UK), post-processing with Meta v23.1.0 (BETA CAE Systems, Luzern, Switzerland) and Matlab R2019b (Mathworks, Nattick, MA, USA). To reach a penetration free state between the occupant models and the seat, the seat foam was deformed in a pre-simulation using the dynamic relaxation option in LS-DYNA, creating stresses and strains in the seat foam but not in the occupant models that were treated as rigid during this phase. All simulations were conducted using 128 AMD EPYC 7532 Central Processing Unit (CPU) cores for 200 ms. A total of eight simulations were run, two with THOR in upright and reclined position, four with the SAFER HBM v10 and v11 upright and reclined, and lastly two repeated simulations of the SAFER HBMs in upright position with the load cells rigidly attached to the sled.

III. RESULTS

The ISO Scores for the verification and validation simulations are summarized in Table I. For the sled model verification simulations with THOR, the boundary conditions had over-all fair correlation (>0.58) while for the kinematics, the average ISO scores were just below the fair rating limit, at 0.55 and 0.56 for the upright and reclined positions, respectively, Table I and Table CI in Appendix C. For the HBM simulation results, the HBMs reached average kinematic ISO scores of 0.55–0.59 in both the upright and reclined positions, while the boundary conditions average ISO scores were higher at 0.65–0.69, Table I and Table CI in Appendix C.

TABLE I. OVERALL AVERAGE ISO SCORES.

Position	**Upright (25°)**			**Reclined (45°)**		
Simulation	1	2	3	4	5	6
Occupant Model Reference tests	FE THOR [27]	SAFER HBM v10 [26]	SAFER HBM v11 [26]	FE THOR [27]	SAFER HBM v10 [26]	SAFER HBM v11 [26]
Kinematics	0.55	0.59	0.58	0.56	0.55	0.56
Boundary Conditions	0.65	0.65	0.66	0.61	0.65	0.68

Of the simulated occupant models, both SAFER HBM v10 and v11 had similar simulation times of approximately 3 h, while the FE THOR simulations took 4 to 4.5 h for 200 ms simulations, on 128 CPU in the modelled sled environment. All eight simulations led to a normal termination at the end of the specified simulation time.

Sled FE Model Verification

The verification simulations with THOR, Fig. 3, showed that the developed sled FE model was able to reproduce the experimental setup with over-all better correlation for the boundary conditions than for the kinematics, Table C1 in Appendix C.

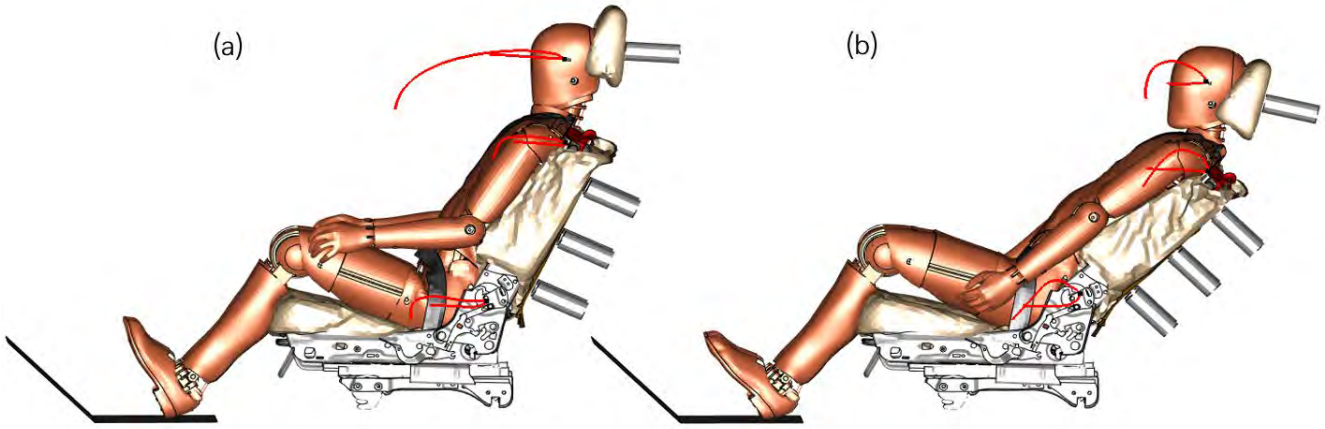

Fig. 3. Snapshot of the THOR simulations in upright (a) and reclined (b) positions at t=50 ms. The red trajectories show the paths of the head, T1 and pelvis in the sled reference frame.

For the major signals in the loading (X) direction, the correlation was high in general. For instance, the head X displacement was Good on the ISO rating scale at 0.9 for the upright, Fig. D1(d) in Appendix D, and Fair at 0.77 for the reclined, Fig. 4(d), THOR simulations compared with the test data. For several of the perpendicular (Z) axis signals, the correlation between simulation and test was considerably lower due to the presence of a Z-direction acceleration component present in the simulations that was missing in the test data, Fig. 4(b). Moreover, the head upward displacement, which had a small magnitude in the test data, was overpredicted for both upright, Fig. D1(e) in Appendix D, and reclined positions, Fig. 4(e).

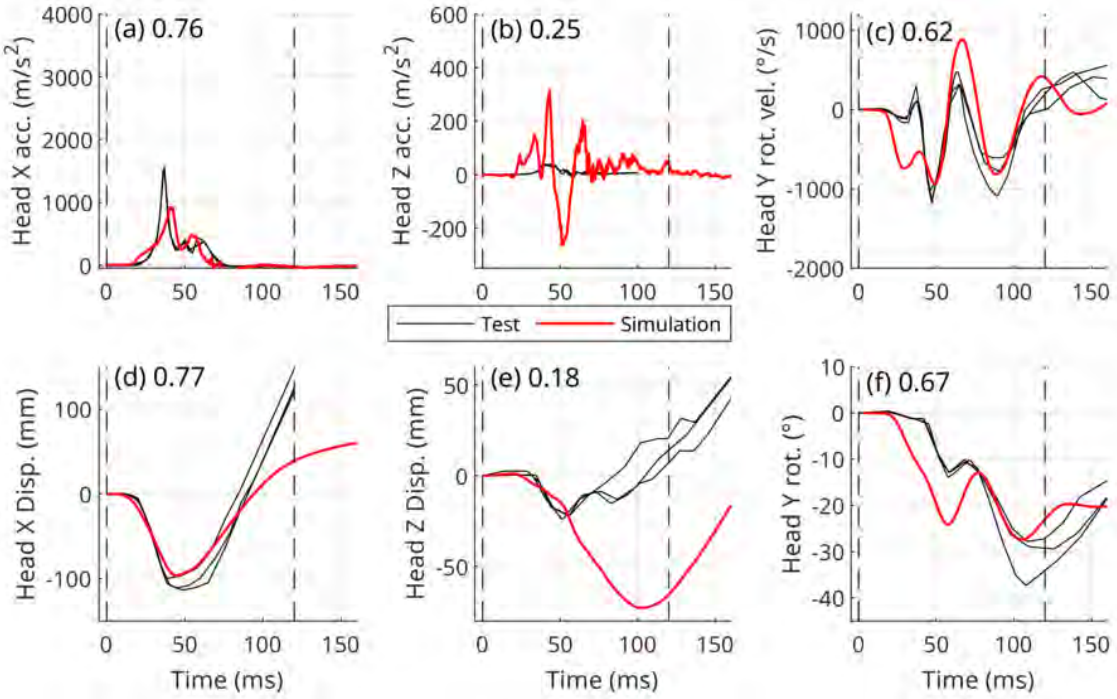

Fig. 4. THOR simulation head kinematics in the reclined (45°) position compared with three tests [27]. The number after the letter notation for each panel is the ISO score, and the time interval used for its calculation is indicated by the dashed lines. Acc. = Acceleration; Disp. = Displacement; Rot. = Rotation; Rot. Vel. = Rotational Velocity.

In general, the seat back and head restraint boundary conditions, Fig. 5 and Fig. E3 in Appendix E, had higher ISO scores than the ATD kinematic signals. The seat back forces matched the test data for the THOR simulations, with ISO scores over 0.63 for all these signals. The head restraint moment and Z force, Fig. 5 and Fig. E3 in Appendix E, received lower ISO scores due to noisy test and simulation results.

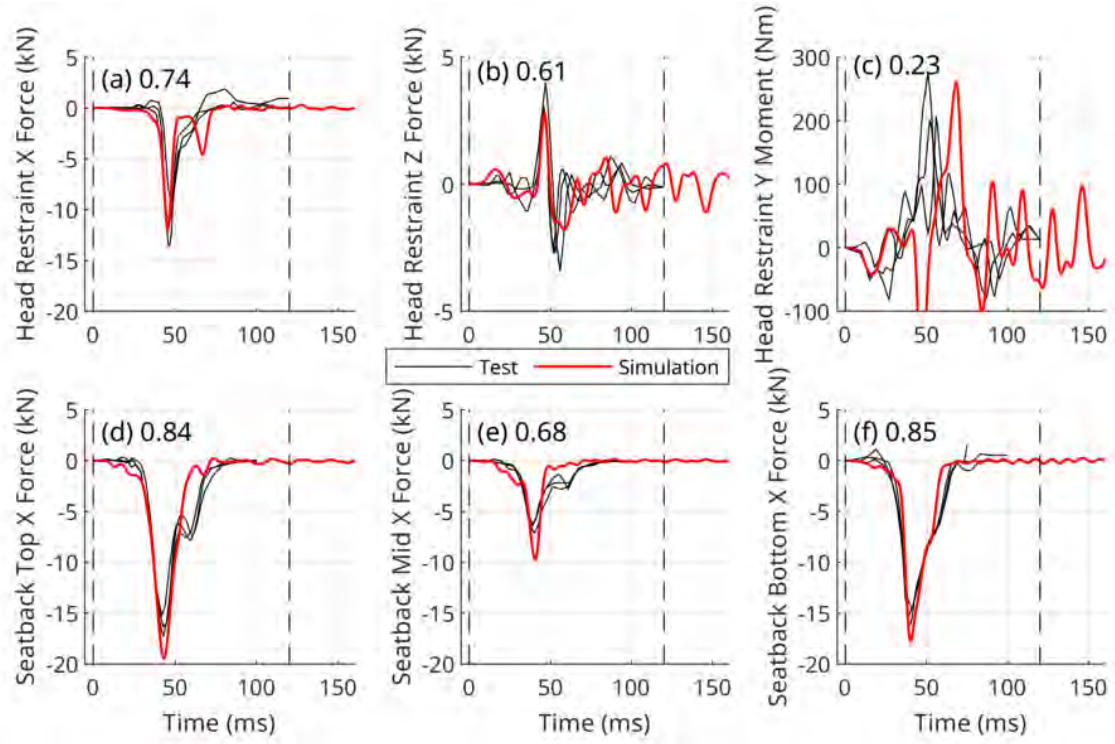

Fig. 5. THOR simulation head restraint and seat back boundary conditions in the upright (25°) position compared with three tests [27]. The number after the letter notation for each panel is the ISO score, and the time interval used for its calculation is indicated by the dashed lines.

HBM Simulation Results

For the first 50 ms of the rear-facing impact simulation, both HBMs moved into the seat in a straight line with the seat in the upright position, Fig. 6, while for the reclined position the head, T1 and pelvis moved slightly upward also during this early phase, similar to the PMHSs in testing. After 50 ms, the head engaged the head restraint, giving an upward and then forward rebound motion of the head, which was also followed by upward and forward motion of the T1 and pelvis for both HBMs in both positions.

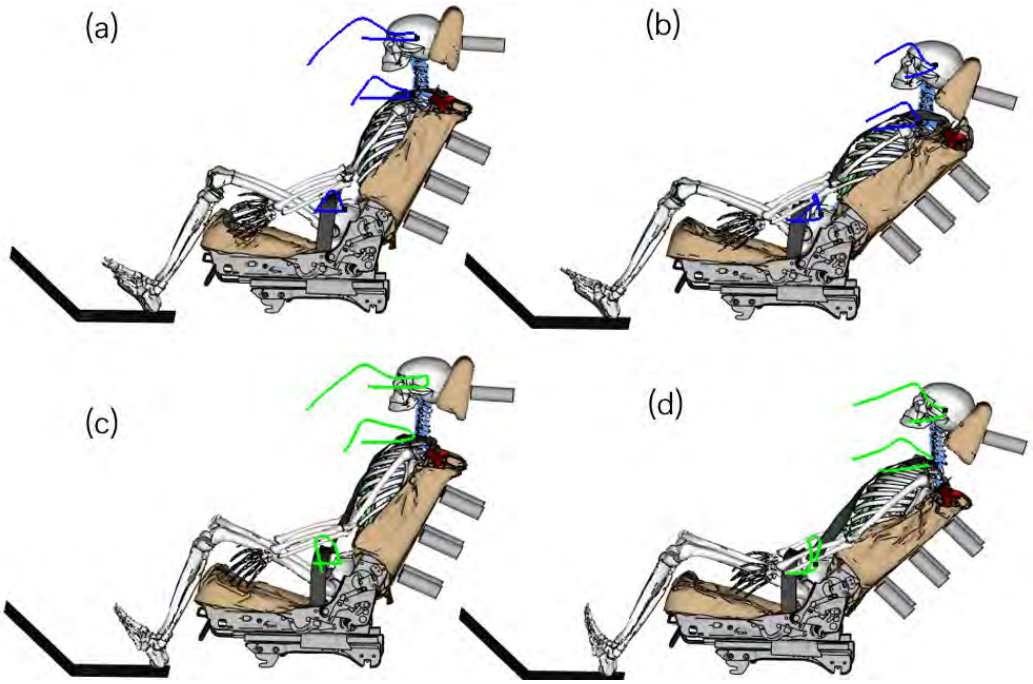

Fig. 6. Snapshots of the SAFER HBM v10 (a, b) and v11 (c, d) in the upright (a, c) and reclined (b, d) position at t=50 ms with soft tissues blanked out to show the skeletal structures. The blue (v10) and green (v11) trajectories show the paths of the head, T1 and pelvis, respectively.

The HBM head kinematics in the upright position, Fig. 7, showed that the interaction with the head restraint had a two-phase response that was not present in the PMHS tests. During the first phase, the HBM heads rotated forward in flexion (negative head rotation), before going into extension that was the major head rotation motion present for the PMHSs before the rebound.

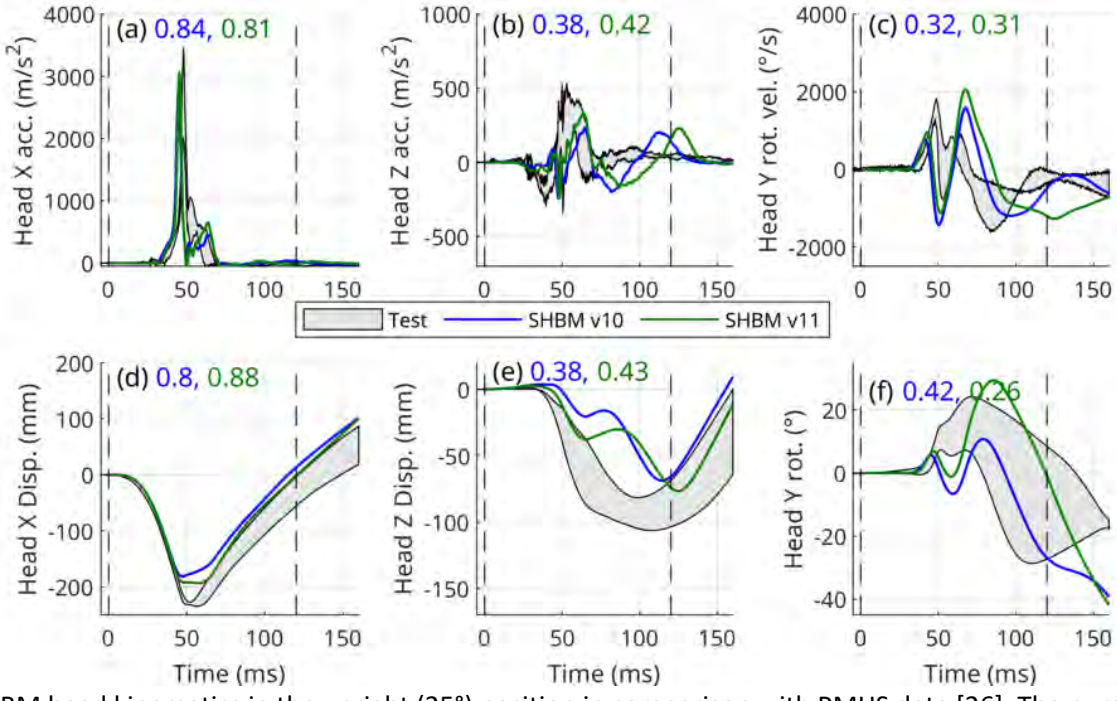

Fig. 7. HBM head kinematics in the upright (25°) position in comparison with PMHS data [26]. The number after the letter notation for each panel is the ISO score, and the time interval used for its calculation is indicated by the dashed lines. Acc. = Acceleration; Disp. = Displacement; Rot. = Rotation; Rot. Vel. = Rotational Velocity.

Moreover, for the upright position, similar to the head X displacement, the T1 X displacement did not reach as far as for the PMHS. However, overall, the T1 X-displacement matched the PMHS data relatively well with ISO Scores of 0.77 and 0.69 for v10 and v11, respectively, Fig. 8(d). SAFER HBM v11 had a higher amplitude T1 Y-rotation, closer to the PMHS response, but a larger overshoot in the rebound response, in total giving a lower ISO score in comparison to the test data than for v10.

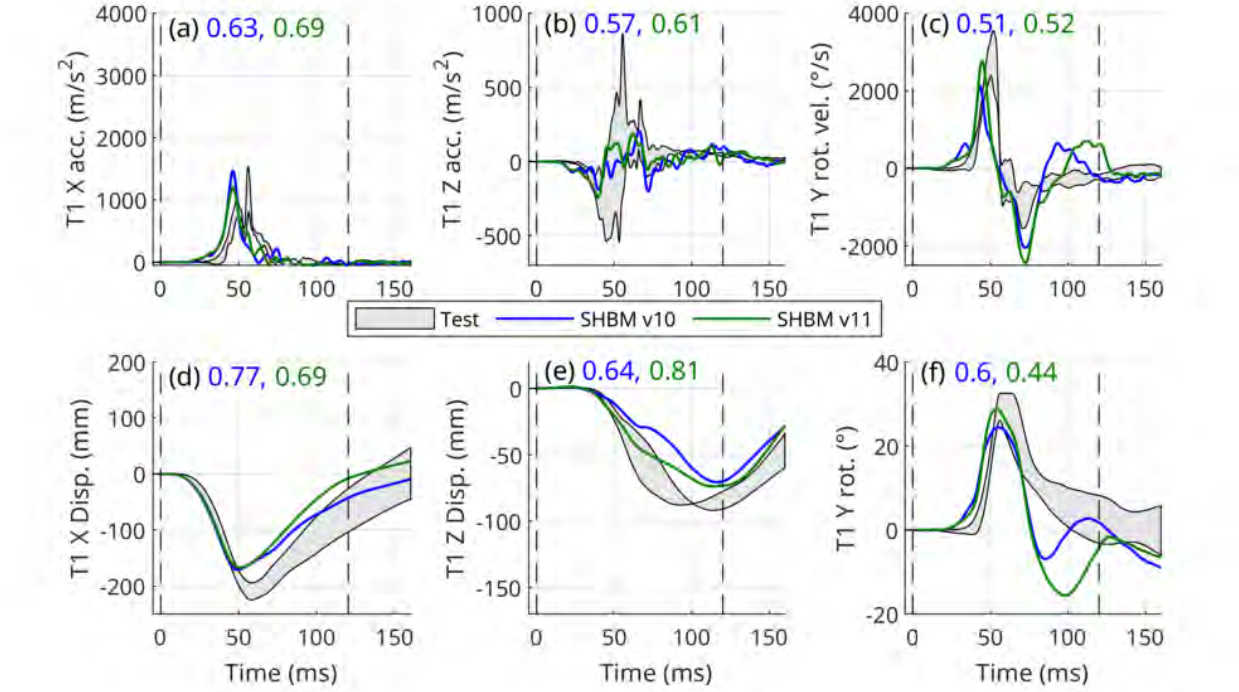

Fig. 8. HBM T1 kinematics in the upright (25°) position in comparison with PMHS data [26]. The number after the letter notation for each panel is the ISO score, and the time interval used for its calculation is indicated by the dashed lines. Acc. = Acceleration; Disp. = Displacement; Rot. = Rotation; Rot. Vel. = Rotational Velocity.

Similar to the head and T1 kinematics, the pelvis X-displacement was limited, and pelvis rotation captured an initial flexion motion of the pelvis present in the PMHS, but did not follow the positive rearward rotation of the pelvis during the rebound phase after about 50 ms for the upright position, Fig. 9(e).

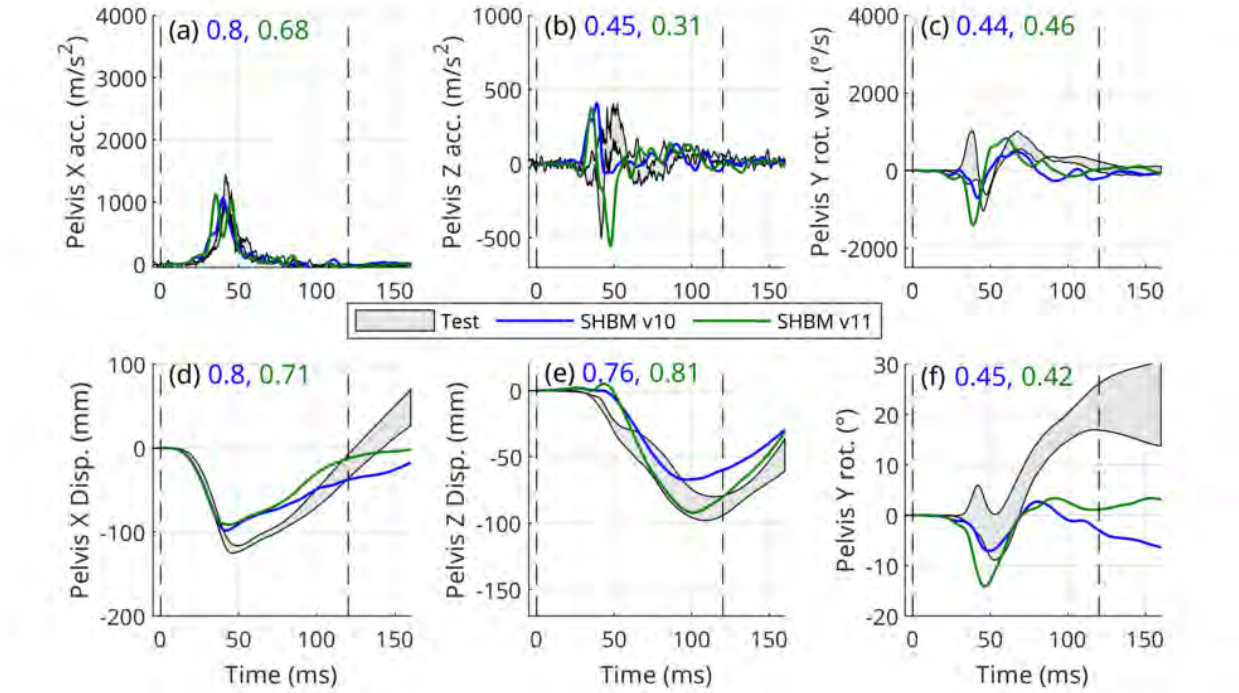

Fig. 9. HBM pelvis kinematics in the upright (25°) position in comparison with PMHS data [26]. The number after the letter notation for each panel is the ISO score, and the time interval used for its calculation is indicated by the dashed lines. Acc. = Acceleration; Disp. = Displacement; Rot. = Rotation; Rot. Vel. = Rotational Velocity.

For the reclined position the PMHS "*climbed*" on the head restraint cushion, tilting the head over backwards into extension. This was not captured by either of the HBMs, Fig. 10(f), for which the heads were pushed into flexion (negative rotation) during the rebound phase starting at around 50 ms. SAFER HBM v11 had marginally closer peak X and Z displacements, as well as some indication of initial head extension motion before rebound, but otherwise ISO scores for head X displacement and head rotation velocity and rotation were low.

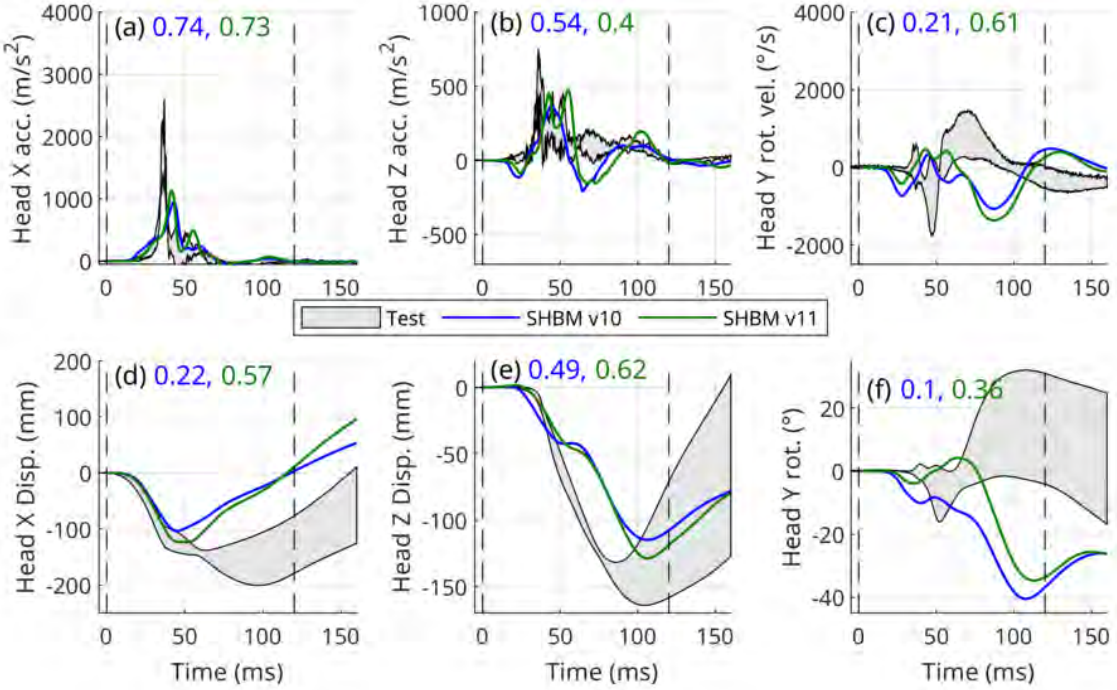

Fig. 10. HBM head kinematics in the reclined (45°) position in comparison with PMHS data [26]. The number after the letter notation for each panel is the ISO score, and the time interval used for its calculation is indicated by the dashed lines. Acc. = Acceleration; Disp. = Displacement; Rot. = Rotation; Rot. Vel. = Rotational Velocity.

For the T1 kinematics in the reclined position, the Z-accelerations, Fig. 11, had low ISO scores. SAFER HBM v11 was closer to the peak X and Z displacements, but the T1 Y-rotation rebound response, most likely driven by the head Y-rotation rebound response, had low ISO scores compared with the PMHS test data.

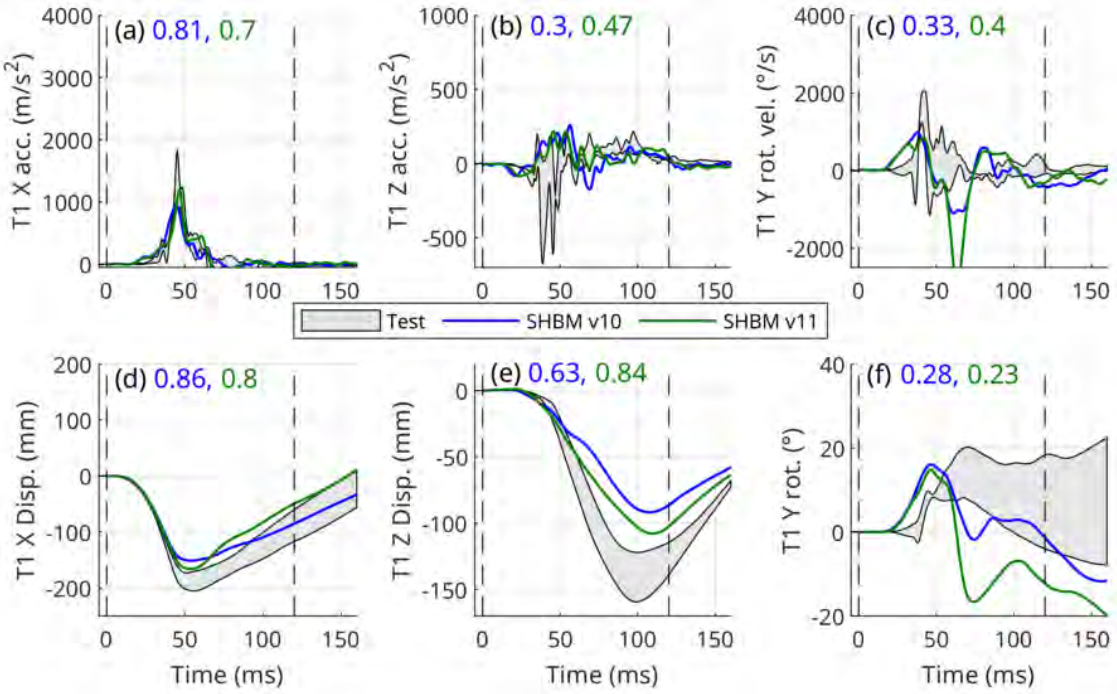

Fig. 11. HBM T1 kinematics in the reclined (45°) position in comparison with PMHS data [26]. The number after the letter notation for each panel is the ISO score, and the time interval used for its calculation is indicated by the dashed lines. Acc. = Acceleration; Disp. = Displacement; Rot. = Rotation; Rot. Vel. = Rotational Velocity.

For the pelvis kinematics in the reclined position, Fig. 12, both HBMs had the same initial negative pelvis Y-

rotation as the PMHS in testing. Still, it did not reach as high positive pelvis Y-rotation angles during the rebound phase after 75 ms. Similar to the PMHS, both HBMs lifted the pelvis, and the ISO scores for the pelvis Z-displacement were 0.80 for SAFER HBM v10, and 0.52 for v11, Fig. 12, respectively.

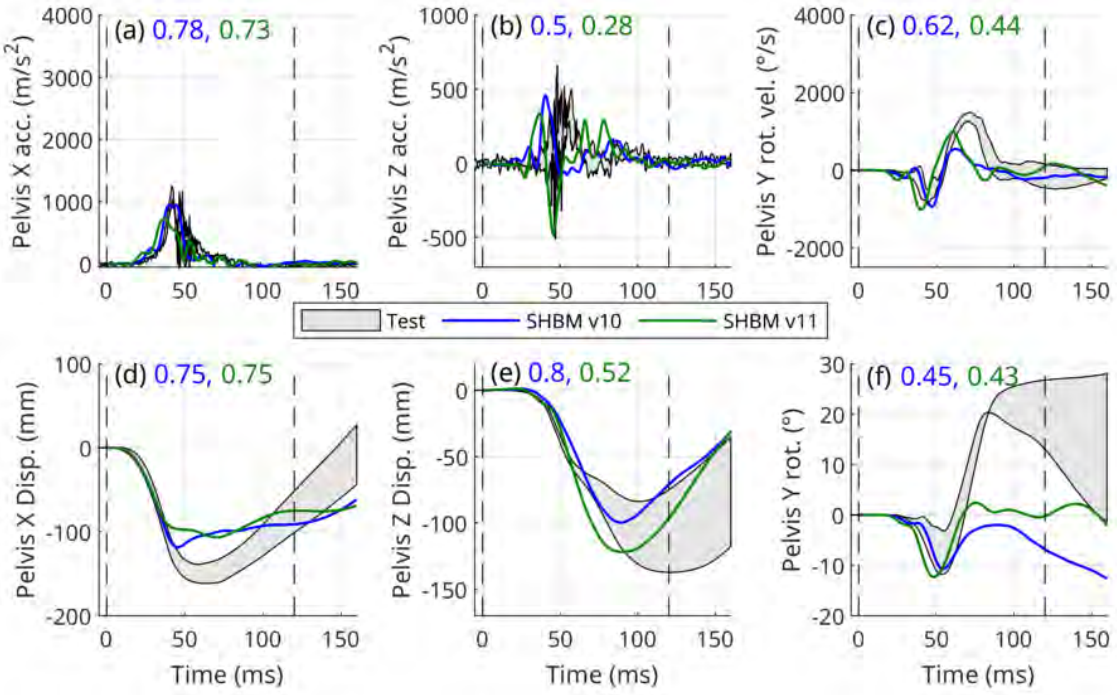

Fig. 12. HBM pelvis kinematics in the reclined (45°) position in comparison with PMHS data [26]. The number after the letter notation for each panel is the ISO score, and the time interval used for its calculation is indicated by the dashed lines. Acc. = Acceleration; Disp. = Displacement; Rot. = Rotation; Rot. Vel. = Rotational Velocity.

IV. DISCUSSION

In this study, the SAFER HBM was validated with respect to high-speed rear-facing frontal impact PMHS tests performed previously [26]. To strengthen the confidence of the FE sled model used for the validation, tests performed with the THOR ATD in the same test setup were simulated first. In the model verification, the FE test setup was shown to reproduce the THOR test results for the boundary conditions with average ISO scores above 0.61, and above 0.55 for the ATD kinematics. Some of the evaluated signals, such as the head restraint Y-moment, received low ISO scores due to differences in phase between signals and relatively noisy test data. Overall, the test setup FE model was able to reproduce the physical tests relatively well as shown by the THOR simulations. To first run verifications simulations and compare with the ATD test results allowed some modifications to be identified and implemented when running the ATD simulations. For instance, such modifications were the addition of an EPP block to increase the load reacted in the mid-seat back, pre-tensioning of the seat belts during the first 20 ms to reduce the amount of slack present in the FE belt routing at start of the simulation, and the introduction of the revolute joint with linear stiffness to reproduce the deflection magnitude present in the physical tests, Fig. B2 in Appendix B. All the presented results (for both ATD and HBM simulations) are from this updated sled model. A previous study [28] similarly tuned the seat model response by optimisation of the seat back foam properties to match Hybrid III tests. Even though the THOR ATD is not a perfect surrogate for the PMHSs, as shown by [27], the size and mass-distribution is close enough to the PMHS to give representative loading that allowed for improvement of the developed FE test setup.

Two versions of the SAFER HBM were validated, v10 [6, 7] and v11 [8]. Both models compared reasonably with respect to the PMHS test data, with average ISO Scores above 0.74 for the X accelerations and displacements. Z-displacements and accelerations had lower scores, partially because of a larger difference in peak value than for the X-signals, but mostly due to shape and phase differences. Y-rotations and rotational velocities had lower ISO-scores and similar to the GHBMC M50-O [28], the pelvis rebound rotation was not captured well by the HBMs. The total kinematic ISO scores were just above the limit for fair (>0.58) according to the ISO/TS 18571 method, at 0.59 and 0.58 for v10 and v11, respectively, in the upright position, while for the reclined position it was just below at 0.55 and 0.56. The weighting of composite signals based on the peak value

in the test data [41] was attempted (results not shown) but did not alleviate the issue with some small magnitude signals reducing the total combined ISO score. The average ISO Scores for the THOR simulations and HBM simulations were of similar magnitude in the range 0.55–0.68. For both simulation series the X-components had relatively high scores, while for the THOR simulations the Z-components had lower scores due to noise in the simulation while for the HBM simulations the lower scores were distributed between Z-components and Y-rotations.

One of the differences between the SAFER HBM v10 and v11 is the new spine and updated buttocks soft tissues which gives v11 a sitting height of approximately 91 cm compared with the previous v10 which was short for a 50th percentile male at 87 cm. The effect of the increased sitting height was counteracted by the positioning of the head restraint that was based on the head location for the test setup. However, the increased Z-displacements for the pelvis, T1 and head made the SAFER HBM v11 be closer to the peak Z-displacements than v10 and was likely resulting from the higher sitting height and a more biofidelic spine. Moreover, the chest band deflections, Fig. F4 in Appendix F and Fig. G4 in Appendix G, correlated better for v10 than for v11 which had increased chest band deflections. In the simulations, the chest band deflection was measured on the skin which shears more in SAFER HBM v11 than in v10, which could be one reason for the recorded increase in in chest band deflection. It is possible that modelling an actual chestband could reduce the measured deflections and improve the correlation.

For the present study, the sled and the seat support structure were chosen to be modelled using deformable steel structures, compared with the previous study [28] which used a rigid constraint. During the modelling process it was found that quite high strength steel (DP800, Table AI in Appendix A) was required to avoid plastic deformations of the support structure during the impact. In addition, comparison of the head restraint and head interaction between simulations and film of the THOR [27] and PMHS [26] tests revealed that there was a considerable movement of the head restraint (on average 45 (SD 15) mm, Appendix B) in the tests, similar as reported by [28]. In the present study, this was incorporated into the simulation setup by a linear elastic revolute joint that provided a deflection of the right magnitude, Fig. B2, which was also responsible for the HBM two phase head Z-displacement and Y-rotation response in the upright position, Fig. 7(d) and (e). While the magnitude of displacement provided by this linear elastic revolute joint was correct, it is likely that this modelling can be improved. The linear stiffness does not capture possible friction processes present in the movement of the head restraint in testing and is likely to provide too large spring-back and affect the rebound of the HBMs' heads.

In two additional simulations (ISO Scores in Table CI in Appendix C) for the upright position the load cells were rigidly attached to the sled, short circuiting the deformable support structure. This led to a decrease in the ISO scores for the head X acceleration and displacement and head Y-rotation response, Table CI in Appendix C, while T1 kinematics in general were improved. The seat back boundary conditions were largely unaffected, which means that the high-speed rear-facing frontal-impact sled tests can be simulated more efficiently with a rigid boundary condition (as done by [28]) between seat back load cells and sled, while the head restraint motion should be modelled.

The high-speed rear-facing frontal impact PMHS tests in upright position were also previously modelled and used to validate the GHBMC M50-O v6.0 HBM [28]. In this previous study, the authors utilized the NHTSA BRS [27] to evaluate the HBM with respect to 22 signals from the PMHS tests, using resultant accelerations in the comparison (while for the present study individual X and Y component signals were used). The authors [28] reported an overall kinematics BRS score of 1.71 and boundary condition BRS score of 1.44, with good biofidelity (low BRS score) for the head and pelvis resultant accelerations, for instance. The authors also reported that upward Z-displacements were underestimated by the HBM. To enable a comparison of the current study with this previous study [28], BRS scores for the SAFER HBM v10 and v11 in the upright position was calculated as well, Table CI–CIV in Appendix C. The underpredicted Z-displacements was also found for the SAFER HBM v10 in the present study which had BRS scores above two for the head, T12 and pelvis Z-displacement. At the same time, the SAFER HBM v11 performed better and had larger Z-displacements with BRS scores below 1.44 for these three signals. It is likely that the updated spine and increased sitting height of the SAFER HBM v11 contributed to this improvement. While it should be remembered that the simulation setups used are not identical, influencing the comparison of the correlation to the test data, overall the two SAFER HBMs performed similar to the average BRS scores reported for the GHBMC model the previous study [28].

Both the SAFER HBM versions in the upright position had 27/35 of the evaluated signals with a BRS score below two, Table CI in Appendix C, and these would therefore be rated as Good [27]. For the ISO scores on the other hand, only 3/35 and 7/35 for v10 and v11, respectively, exceeded the limit for Good of 0.8 on the ISO/TS 18571 rating scale. Including also Fair (>0.58) as an acceptable model response, 25/35 and 24/35 signals exceeded this for v10 and v11, respectively, illustrating that the ISO rating scale is much more conservative than the BRS score threshold of 2 proposed by [27]. Notable disagreements between the ISO rating and the BRS score was for the seat back top and middle force, which was rated with high ISO scores of 0.89 and 0.71 for SAFER HBM v11, while having BRS scores of 2.2 and 3.06. These signals had small SD corridors for the test data, making a small deviation of the model response give a poor BRS score. Future comparisons of the BRS and ISO method are encouraged to further understand the relationship between the two methods.

For future vehicles, a user expectation of novel seating positions such as reclined, resting positions, has been identified [9–11]. Such developments create a need for further development of occupant surrogate models such as ATDs and HBMs. As shown in the study with the THOR-50M ATD [27], the THOR was unsuccessful in reproducing the vertical spine motion of the PMHS and pelvis motions in the upright position. The BRS score for both the SAFER HBMs in this study and the GHBMC v6.0 [28] was lower than those of THOR for the head and pelvis kinematics, Table CIV in Appendix C, indicating the potential for HBMs as occupant surrogates with better biofidelity than the THOR ATD in high-speed rear-facing frontal impacts as simulated here.

V. CONCLUSION

In this study, both the SAFER HBM v10 and v11 was found to compare reasonably with respect to high-speed rear-facing frontal impact PMHS test data, with average ISO Scores above 0.74 for X accelerations and displacements. Z-displacements and accelerations had lower scores, partially because of a larger difference in peak value than for the X-signals, but mostly due to shape and phase differences. The SAFER HBM v11 showed better biofidelity with respect to Z-displacements, which was highlighted in previous work as challenging both for the THOR-50M ATD in physical testing and the GHBMC M50-O in simulations in the upright position. Before running the HBM validation simulations, tests performed with THOR in the same test setup as used for the PMHS tests was simulated and enabled development of the test setup FE model without tuning it with respect to the HBM simulation results. The potential of HBMs for evaluation of novel seating positions was demonstrated for rear-facing occupants in high-speed frontal impacts and in reclined positions.

VI. ACKNOWLEDGMENTS

This work was carried out at SAFER, Vehicle and Traffic Safety Centre at Chalmers University of Technology, Gothenburg, Sweden, and funded by FFI-Strategic Vehicle Research and Innovation, by Vinnova, the Swedish Energy Agency, the Swedish Transport Administration and the Swedish vehicle industry.

VII. REFERENCES

[1] Davis, M., Koya, B., Schap, J. M., Gayzik, F. S. (2016) Development and Full Body Validation of a 5th Percentile Female Finite Element Model. *Stapp Car Crash Journal,* **60**: pp.509–544.

[2] Davis, M. L., Vavalle, N. A., Gayzik, F. S. (2015) An Evaluation of Mass-Normalization using 50th and 95th Percentile Human Body Finite Element Models in Front Crash. *Proceedings of the IRCOBI Conference*, Lyon, France.

[3] Park, G., Kim, T., *et al.* (2014) Evaluation of the Biofidelity of the Finite Element 50th Percentile Male Human Body Model (GHBMC) under Lateral Shoulder Impact Conditions. *Proceedings of the IRCOBI Conference*, Berlin, Germany.

[4] Schwartz, D., Guleyupoglu, B., Koya, B., Stitzel, J.D., Gayzik, F.S. (2015) Development of a Computationally Efficient Full Human Body Finite Element Model. *Traffic Injury Prevention,* **16**(Sup1): pp.S49–56.

[5] Watanabe, R., Katsuhara, T., Miyazaki, H., Kitagawa, Y., Yasuki, T. (2012) Research of the Relationship of Pedestrian Injury to Collision Speed, Car-type, Impact Location and Pedestrian Sizes using Human FE model (THUMS version 4). *Stapp Car Crash Journal,* **56**: pp.269–321.

[6] Pipkorn, B., Östh, J., *et al.* (2021) Validation of the SAFER Human Body Model Kinematics in Far-Side Impacts. *Proceedings of the IRCOBI Conference*, Online.

[7] Östh, J., Pipkorn, B., Iraeus, J., Forsberg, J. (2021) Numerical Reproducibility of Human Body Model Crash Simulations. *Proceedings of the IRCOBI Conference,* Online.

[8] John, J., et al. (In preparation) Development of SAFER HBM v11. Zenodo. https://doi.org/10.5281/zenodo.10886711

[9] Jin X, Hou H, Shen M, Wu H, Yang KH. (2018) Occupant Kinematics and Biomechanics with Rotatable Seat in Autonomous Vehicle Collision: A Preliminary Concept and Strategy. *Proceedings of the IRCOBI Conference,* Athens, Greece.

[10] Jorlöv S, Bohman K, Larsson A. (2017) Seating Positions and Activities in Highly Automated Cars – A Qualitative Study of Future Automated Driving Scenarios. *Proceedings of the IRCOBI Conference*, Antwerp, Belgium.

[11] Östling M, Larsson A. (2019) Occupant Activities and Sitting Positions in Automated Vehicles in China and Sweden. *Proceedings of the ESV Conference*, Paper no. 19-0083, Eindhoven, The Netherlands.

[12] Forman JL, Kent RW, Mroz K, Pipkorn B, Bostrom O, Segui-Gomez M. (2012) Predicting Rib Fracture Risk with Whole-Body Finite Element Models: Development and Preliminary Evaluation of a Probabilistic Analytical Frame Work. *Annals of Advances in Automotive Medicine*, **56**:109–124

[13] Hayes, A.R., Vavalle N.A., Moreno, D.P., Stitzel J.D., Gayzik S.C. (2014) Validation of Simulated Chestband Data in Frontal and Lateral Loading Using a Human Body Finite Element Model. *Traffic Injury Prevention* 15(2): 181–186.

[14] Östh, J., Mendoza-Vazquez, M., Linder, A., Svensson, M.Y., Brolin, K. (2017) The VIVA OpenHBM Finite Element 50th Percentile Female Occupant Model: Whole Body Model Development and Kinematic Validation. *Proceedings of the IRCOBI Conference*, Antwerp, Belgium.

[15] Pipkorn, B., Iraeus, J., Björklund, M., Bunketorp, O., Jakobsson, L. (2019) Multi-scale Validation of a Rib Fracture Prediction Method for Human Body Models. *Proceedings of the IRCOBI Conference*, Florence, Italy.

[16] Larsson, K.J., Pipkorn, B., Iraeus, J., Bolte, J.H., Agnew, A.M., Hu, J., Reed, M.P (2019) Evaluation of the benefits of parametric human body model morphing for prediction of injury to elderly occupants in side impact. *Proceedings of the IRCOBI Conference*, Florence, Italy.

[17] Hwang, E., Hu, J., Reed, M.P. (2020) Validating Diverse Human Body Models Against Side Impact Tests with Post-Mortem Human Subjects. *Journal of Biomechanics* **98**: 109444.

[18] Gepner, B.D., Perez-Rapela, D., Forman, J.L., Östling, M., Pipkorn, B., Kerrigan J.R. (2022) Evaluation of GHBMC, THUMS and SAFER Human Body Models in Frontal Impacts in Reclined Postures. *Proceedings of the IRCOBI Conference,* Porto, Portugal.

[19] Matsuda, T., Kobayashi, N., Fujita, N., Kitagawa, Y. (2023) Development of a Human Body Model (THUMS Version 7) to Simulate Kinematics and Injuries of Reclined Occupants in Frontal Collisions. *Proceedings of the ESV Conference*, Yokohama, Japan.

[20] Yoganandan, N. *et al.* (2000) Biomechanics of Human Occupants in Simulated Rear Crashes: Documentation of Neck Injuries and Comparison of Injury Criteria. *Stapp Car Crash Journal* **44**: 2000-01-SC14.

[21] White, N.A., et al. (2009) Investigation of Upper Body and Cervical Spine Kinematics of Post-Mortem Human Subjects (PMHS) during Low-Speed, Rear-End Impacts. *Stapp Car Crash Journal* **53**: 2009-01-0387.

[22] Kallieris, D., Rizzetti, A., Mattern, R., Thunnissen, J., Phillipens, M. (1996) Cervical Human Spine Loads During Traumatomechanical Investigations. *Proceedings of the IRCOBI Conference,* Dublin, Ireland.

[23] Kang, Y.-S., Bolte, J.H., Moorhouse, K., Donnelly, B., Herriott, R., Mallory, A. (2012) Biomechanical Responses of PMHS in Moderate-Speed Rear Impacts and Development of Response Targets for Evaluating the Internal and External Biofidelity of ATDs. *Stapp Car Crash Journal* **56**: 105–170.

[24] John, J.D., Putra, I.P.A., Iraeus, J. (2022) Finite Element Human Body Models to Study Sex-differences in Whiplash Injury: Validation of VIVA+ Passive Response in Rear-Impact. *Proceedings of the IRCOBI Conference,* Porto, Portugal.

[25] Katagiri, M., Zhay, J., Lee, S., Moorhouse, K., Kang, Y.-S. (2019) Biofidelity Evaluation of GHBMC Male Occupant Models in Rear Impacts. *Proceedings of the IRCOBI Conference,* Florence, Italy.

[26] Kang, Y.-S., Stammen, J., Ramachandra, R., Agnew, A.M., Hagedorn, A., Thomas, C., Kwon H.Y., Moorhouse, K., Bolte J.H. IV (2020) Biomechanical Responses and Injury Assessment of Post Mortem Human Subjects in Various Rear-facing Seating Configuration. *Stapp Car Crash Journal* **64**: 155–212.

[27] Hagedorn, A., Stammen, J., Ramachandra, R., Rhule, H., Thomas, C., Suntay, B., Kang, Y.-S., Kwon, H.J., Moorhouse, K., Bolte J.H. IV (2022) Biofidelity Evaluation of THOR-50M in Rear-Facing Seating Configurations Using and Updated Biofidelity Ranking System. S*AE International Journal of Transportation Safety* **10**(2): 291–375.

[28]Pradhan, V.V., Ramachandra, R., Stammen, J., Kracht, C., Moorhouse, K., Bolte, J.H., Kang, Y.-S. (2023) Biofidelity Assessment of the GHBMC M50-O in a Rear-Facing Seat Configuration during High-Speed Frontal Impact. *Computer Methods in Biomechanics and Biomedical Engineering*, 1–16.

[29]Bridges, W., Ganesan, V., Barki, G., Jayakumar, P., Davies, Y., Umashankar, S.M.K. (2022) *Integrated Seat Belt System Model Development*. Report No. DOT HS 813 116. National Highway Traffic Safety Administration, Washington, USA.

[30]NHTSA (2023) Crash Simulation Vehicle Models. https://www.nhtsa.gov/crash-simulation-vehicle-models. Accessed in January 2023.

[31]Markert B (2005) *Porous Media Viscoelasticity with Application to Polymeric Foams*. PhD Thesis, University of Stuttgart, Germany.

[32]Untaroiu, C.D., Shin, J., Crandall, J.R., Fredriksson, R., Boström, O., Takahashi, Y., Akiyama, A., Okamoto, M., Kikuchi, Y. (2010) Development and Validation of Pedestrian Sedan Bucks using Finite-Element Simulations: A Numerical Investigation of the Influence of Vehicle Automatic Braking on the Kinematics of the Pedestrian Involved in Vehicle Collisions. *International Journal of Crashworthiness* **15**(5): 491–503.

[33]Iraeus, J., Pipkorn, B. (2019) Development and Validation of a Generic Finite Element Ribcage to be Used for Strain-based Fracture Prediction. *Proceedings of the IRCOBI Conference*, Florence, Italy.

[34]Brynskog, E., Iraeus, J., Reed, M.P., Davidsson, J. (2021) Predicting Pelvis Geometry using a Morphometric Model with Overall Anthropometric Variables. *Journal of Biomechanics* **126**: 110633.

[35]Pipkorn, B., Iraeus, J., Björklund, M., Bunketorp, O., Jakobsson, L. (2019) Multi-Scale Validation of a Rib Fracture Prediction Method for Human Body Models. *Proceedings of the IRCOBI Conference*, Florence, Italy.

[36]Kleiven, S. (2007) Predictors for Traumatic Brain Injuries Evaluated through Accident Reconstructions. *Stapp Car Crash Journal*, 51.

[37]Iraeus, J., Niranjan Poojary, Y., Jaber, L., John, J., Davidsson, J. (2023) A New Open-Source Finite Element Lumbar Spine Model, its Tuning and Validation, and Development of a Tissue-based Injury Risk Function for Compression Fractures. *Proceedings of the IRCOBI Conference*, Cambridge, England.

[38]Östh, J., Brolin, K., Svensson, M.Y., Linder, A. (2016) A Female Ligamentous Cervical Spine Finite Element Model Validated for Physiological Loads. *Journal of Biomechanical Engineering* **138**(6): 061005.

[39]ISO (2014) *ISO/TS 18571 Road Vehicles – Objective Rating Metric for Non-ambigous Signals*. International Standard Organisation, Geneva, Switzerland.

[40]Society of Automotive Engineers (2007) *SAE J211-1 Instrumentation for Impact Test, Surface Vehicle Recommended Practice*. Society of Automotive Engineers, Warrendale, PA, USA.

[41]Klug, C., Schachter, M., Eggers, A., Galazka, J., Gargallo, S., Jimenez, C., Kirch, J., Levallois, I., Loebenwein, U., Meissner, N., Pardede, V., Pipkorn, B., Ellway, J., van Ratingen, M. (2023) Euro NCAP Virtual Testing – Crashworthiness. *Proceedings of the ESV Conference*, Yokohama, Japan.

VIII. APPENDIX A – SLED FE DETAILS

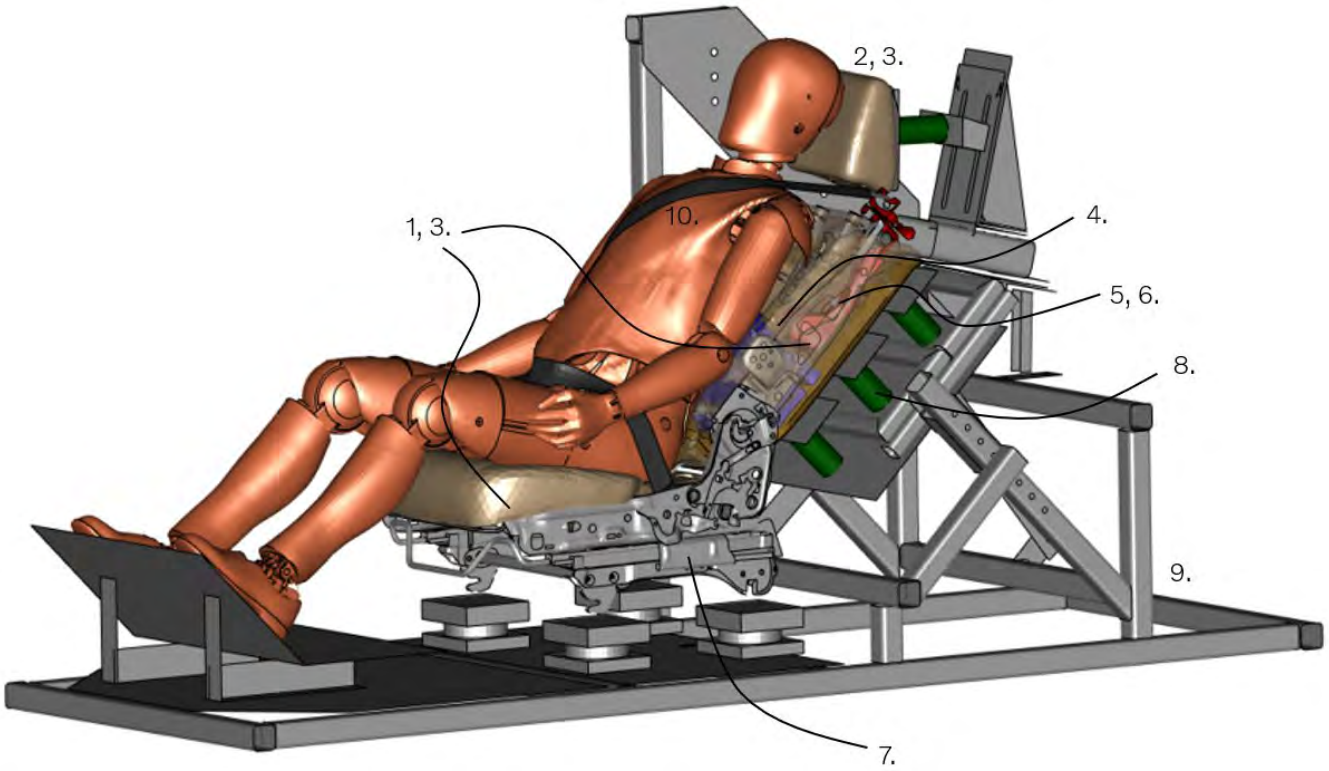

Fig. A1. The FE sled test setup with the THOR-50M FE model in the reclined position with 45° seat back angle.

TABLE AI. MATERIALS USED FOR THE FE SLED TEST SETUP. NO. = NUMBERS REFERRING TO FIG. A1.

No.	Part(s)	Element Type (ELFORM)	Characteristic Element Length (mm)	Material Model (*MAT_no)	Material Parameters	Shell Thickness (mm)	Reference
1	Cushion and back rest foam	Tetrahedral (10)	15	FU_CHANG_FOAM (83)	E=0.138 MPa, DAMP=0.05, RO=0.048 kg/m^3	N/A	[31]
2	Head restraint foam	Tetrahedral (10)	10	FU_CHANG_FOAM (83)	E=0.69 MPa, DAMP=0.05, RO=0.0103 kg/m3	N/A	[31]
3	Cushion, back rest, head restraint outer surface	Triangular membrane (9)	10–15	PIECEWISE_LINEAR_PLASTICITY (24)	E=5.5 GPa, v=0.3, σ_{max}=22 MPa	0.6	[29]
4	Seat back EPP Insert	Tetrahedral (10)	15	FU_CHANG_FOAM (83)	E=10 MPa, DAMP=0.05, RO=0.1 kg/m^3	N/A	[32]
5	Retractor Cover	Full-integrated quadrilateral (16)	7	HDPE, MODIFIED_PIECEWISE_LINEAR (123)	E=1.2 GPa, v=0.3, σ_{max}=30 Mpa, RO=0.95 kg/m^3	2	[29]
6	Retractor	Quadrilateral (1)	7	RIGID (20)	N/A	0.6	None
7	Seat frame	Full-integrated quadrilateral (16)	7	High, mid and low strength steels, MODIFIED_PIECEWISE_LINEAR (123)	E=210 GPa, v=0.3, RO=7.86 kg/m^3	1–5.04	[29]
8	Load cells	Full-integrated selective reduced hexahedral solid (2)	7	Low strength steels, MODIFIED_PIECEWISE_LINEAR (123)	E=210 GPa, v=0.3, RO=4.23 kg/m^3	N/A	None
9	Sled structural parts	Full-integrated quadrilateral (16)	10	High strength (DP800) steel, MODIFIED_PIECEWISE_LINEAR (123)	E=210 GPa, v=0.3, RO=7.86 kg/m^3	1.0–12.7	[29]
10	Seat Belt	1 D and 2 D seat belt elements	12	Webbing material with 7% elongation at 11 kN. MAT_SEATBELT (B01)		1.25	[29]

TABLE AII. POSITIONING DATA FOR THE THOR-50M FE MODEL RELATIVE TO THE POSITION IN THE PHYSICAL TESTS [27].

Position	Head Angle (°)	Pelvis Angle (°)	Thigh Angle (°)	Leg Angle (°)	Hip-to-Eye Angle (°)	Backset (mm)	Topset (mm)
FE THOR, Upright	0.0	30.4	11.5	52	13.4	85	85
Test mean [27]	0.2	30.3	12.3	51.1	13.5	85.6	80
Test S.D. [27]	0.6	1.2	1.4	1.4	0.6	2.5	5.0
FE THOR, Reclined	24.2	30.9	11.0	53.0	31	0	85
Test mean [27]	23.9	30.9	11.0	51.1	28.0	0	80
Test S.D. [27]	0.7	0.6	0.6	1.6	0.5	0	5.0

TABLE AIII. POSITIONING DATA FOR THE SAFER HBM V10 AND V11 MODELS RELATIVE TO THE POSITION IN THE PHYSICAL TESTS [26]. N.A. = NOT AVAILABLE.

Position	Head Angle (°)	Pelvis Angle (°)	Thigh Angle (°)	Leg Angle (°)	Hip-to-Eye Angle (°)	Backset (mm)	Topset (mm)
SAFER HBM v10, Upright	0.3	35.9	16.8	36.7	8.0	85	105
SAFER HBM v11, Upright	2.9	45.2	15.2	39.3	8.6	85	105
Test mean [26]	0.1	32.1	12.6	42.4	7.0	79.3	N.A.
Test S.D. [26]	1.7	3.0	1.1	2.9	2.0	4.5	N.A.
SAFER HBM v10, Reclined	28.1	23.6	15.2	40.9	30.5	0	105
SAFER HBM v11, Reclined	28.6	39.4	11.8	49.2	27.6	0	105
Test mean [26]	27.5	29.2	11.7	42.1	28.8	0	N.A.
Test S.D. [26]	4.9	9.0	1.8	3.4	2.5	0	N.A.

IX. APPENDIX B – HEAD RESTRAINT DYNAMIC DEFLECTION IN PHYSICAL TESTS AND SIMULATIONS

In the physical tests with the PMHS [26] and THOR [27], there was considerable dynamic deflection motion of the head restraint in all tests. For the present study, the head restraint deflection was quantified in the sled onboard X-Z coordinate system by tracking the top Patrick-marker of the head restraint mount, Fig. B1, in a dynamic coordinate system attached to the background screen travelling with the sled in Meta v23.1.0 (BETA CAE Systems, Luzern, Switzerland) using length of the bottom of the head restraint plate (90 mm) for scaling.

Fig. B1. Tracking of the top head restraint mounting bracket Patrick-marker in Meta for the THOR-729 upright test [27]. The green trace shows the dynamic motion of the marker and head restraint during the test, with a peak deflection of 41 mm in the negative X-direction.

The average dynamic deflection of the top head restraint Patrick-marker was 45 mm with a standard deviation 15 mm for a total of 12 tests (6 PMHS, 6 THOR) in both upright and reclined positions, Fig. B2.

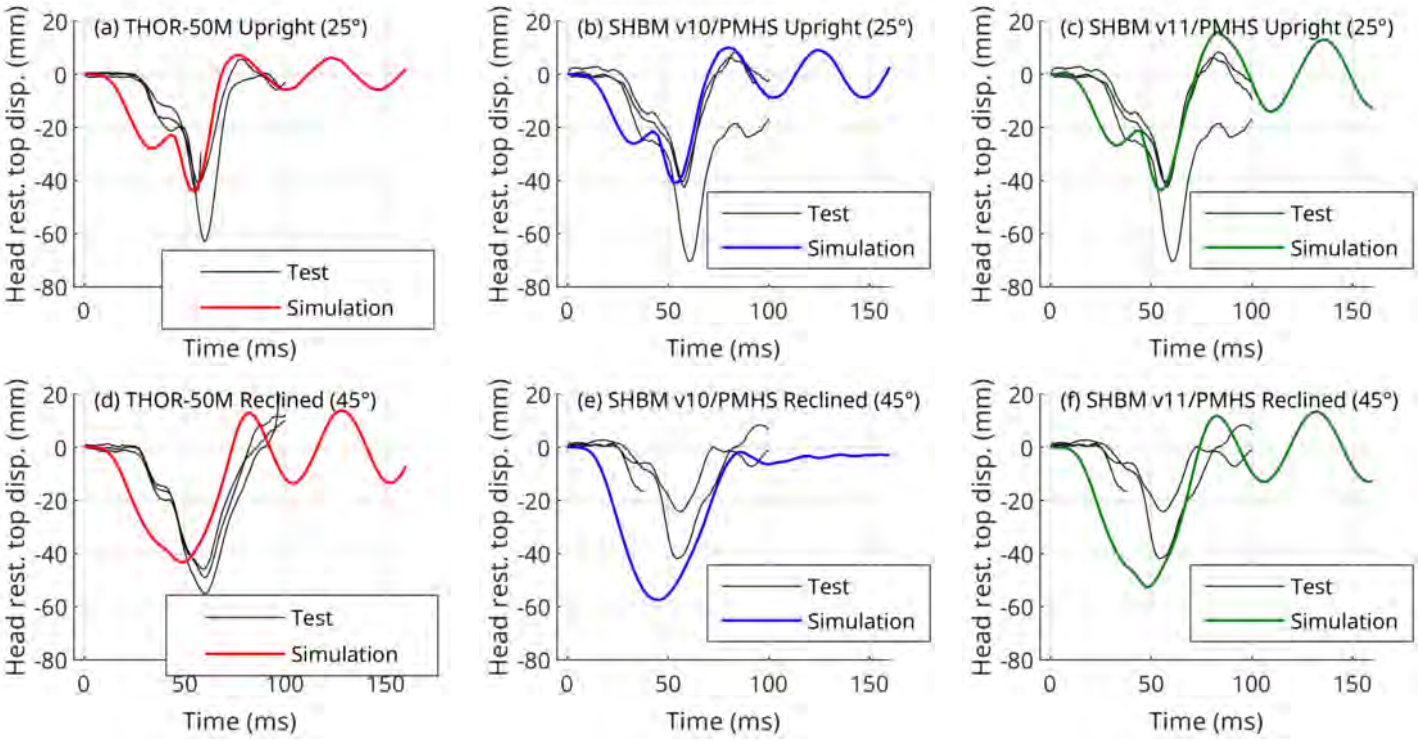

Fig. B2. Dynamic displacement of the head restraint top Patrick-marker, Fig. B1, for the THOR tests (a, d) and for the PMHS tests (b,c,e,f) compared with the response in the FE simulations.

X. APPENDIX C – ISO AND BRS SCORES

TABLE CI. ISO AND BRS SCORES FOR ALL SIMULATIONS.

Position	**Upright (25°)**							**Reclined (45°)**		
Model Reference tests	FE THOR [27]	SHBM v10 [26]	SHBM v11 [26]	SHBM v10 - Rigid BC [26]	SHBM v11 - Rigid BC [26]	SHBM v10 - BRS [26]	SHBM v11 - BRS [26]	FE THOR [27]	SHBM v10 [26]	SHBM v11 [26]
Head X Disp.	0.90	0.80	0.88	0.74	0.76	1.82	1.29	0.77	0.22	0.57
Head Z Disp.	0.17	0.38	0.43	0.43	0.69	2.14	1.40	0.18	0.49	0.62
Head X Acc.	0.76	0.84	0.81	0.75	0.76	0.97	1.27	0.76	0.74	0.73
Head Z Acc.	0.17	0.38	0.42	0.42	0.37	1.10	1.11	0.25	0.54	0.40
Head Y Rot. Vel.	0.66	0.32	0.31	0.26	0.27	1.81	2.85	0.62	0.21	0.61
Head Y Rot.	0.64	0.42	0.26	0.28	0.38	1.02	1.16	0.67	0.10	0.36
T1 X Disp.		0.77	0.69	0.82	0.74	0.76	1.38		0.86	0.80
T1 Z Disp.		0.64	0.81	0.67	0.90	2.52	1.44		0.63	0.84
T1 X Acc.	0.71	0.63	0.69	0.62	0.76	1.71	1.31	0.72	0.81	0.70
T1 Z Acc.	0.34	0.57	0.61	0.52	0.58	0.64	0.66	0.26	0.30	0.47
T1 Y Rot. Vel.	0.80	0.51	0.52	0.58	0.67	2.21	2.10	0.63	0.33	0.40
T1 Y Rot.		0.60	0.44	0.67	0.72	1.04	1.75		0.28	0.23
T4 X Acc.	0.65	0.76	0.73	0.79	0.78	1.66	1.21	0.66	0.72	0.75
T4 Z Acc.	0.30	0.51	0.37	0.39	0.39	0.87	1.02	0.30	0.60	0.40
T4 Y Rot. Vel.	0.65	0.62	0.68	0.58	0.62	1.51	1.06	0.57	0.55	0.57
T8 X Acc.		0.78	0.77	0.78	0.77	1.24	0.91		0.70	0.71
T8 Z Acc.		0.56	0.67	0.61	0.62	1.03	0.85		0.69	0.64
T12 X Acc.	0.60	0.68	0.69	0.69	0.71	1.40	1.00	0.59	0.65	0.62
T12 Z Acc.	0.25	0.71	0.78	0.72	0.75	1.05	0.68	0.29	0.77	0.75
T12 Y Rot. Vel.	0.23	0.33	0.37	0.41	0.44	1.70	1.85	0.57	0.10	0.32
Pelvis X Disp.	0.39	0.80	0.71	0.79	0.72	2.37	2.27	0.87	0.75	0.75
Pelvis Z Disp.	0.62	0.76	0.81	0.75	0.82	2.08	1.28	0.69	0.80	0.52
Pelvis X Acc.	0.81	0.80	0.68	0.78	0.75	0.92	1.63	0.79	0.78	0.73
Pelvis Z Acc.	0.31	0.45	0.31	0.45	0.29	0.71	1.31	0.25	0.50	0.28
Pelvis Y Rot. Vel.	0.87	0.44	0.46	0.46	0.44	1.48	1.29	0.65	0.62	0.44
Pelvis Y Rot.	0.81	0.45	0.42	0.45	0.42	3.37	3.04	0.58	0.45	0.43
Chestband Defl.		0.54	0.45	0.46	0.36	1.58	2.64		0.53	0.38
Headrestr. X Force	0.74	0.73	0.72	0.66	0.66	1.58	1.70	0.78	0.65	0.72
Headrestr. Z Force	0.61	0.29	0.25	0.43	0.45	1.98	2.50	0.53	0.27	0.35
Headrestr. Y Moment	0.23	0.46	0.28	0.41	0.30	1.13	1.47	0.51	0.29	0.43
Seatback Top X Force	0.84	0.89	0.88	0.84	0.84	2.20	2.05	0.71	0.79	0.82
Seatback Mid X Force	0.68	0.66	0.71	0.76	0.79	3.06	2.79	0.63	0.82	0.81
Seatback Bottom X Force	0.85	0.91	0.93	0.88	0.92	1.68	1.48	0.74	0.92	0.91
Shoulder Belt Force	0.66	0.68	0.68	0.56	0.54	1.57	1.26	0.19	0.76	0.76
Lap Belt Force	0.58	0.62	0.84	0.65	0.84	0.71	0.70	0.80	0.70	0.64
Kinematics	0.55	0.59	0.58	0.59	0.61	1.51	1.47	0.56	0.55	0.56
Boundary Conditions	0.65	0.65	0.66	0.65	0.67	1.74	1.74	0.61	0.65	0.68

TABLE CII. SUMMARY OF BIOFIDELITY RANK SYSTEM (BRS) CALCULATIONS INCLUDING METHOD OF ALIGNMENT FOR DUMMY CURVES (ADAPTED FROM [27]), SAFER HBM BRS SCORE, TIME DURATION FOR BRS CALCULATION, ABSOLUTE VALUE OF DUMMY PHASE SHIFT (DPS) AND AVERAGE AND MAXIMUM OF ABSOLUTE VALUES OF PMHS SHIFT FOR OCCUPANT KINEMATICS. DCAD = DUMMY CUMULATIVE ABSOLUTE DIFFERENCE.

Body region	Occupant kinematics	Method of dummy curve alignment	BRS score (v10/v11)	Time duration for BRS calculation (ms)	Absolute value of DPS (ms) (v10/v11)	Avg. of absolute value of PMHS shift (ms)	Max. of absolute value of PMHS shift (ms)
Head	X-acceleration	Minimum DCAD	0.97/1.27	100	3.15/2.75	1.97	2.95
	Z-acceleration	Minimum DCAD	1.10/1.11	100	8.55/5.00		
	Y-rotation	None	1.02/1.16	160	0.00/0.00		
	Y-angular velocity	None	1.81/2.85	160	0.00/0.00		
	X-displacement	Minimum DCAD*	1.82/1.29	160	0.00/0.60		
	Z-displacement	Minimum DCAD**	2.14/1.40	160	12.70/5.95		
T1	X-acceleration	Minimum DCAD	1.71/1.31	100	8.10/7.35	2.65	3.95
	Z-acceleration	Minimum DCAD	0.64/0.66	100	0.00/0.00		
	Y-rotation	Minimum DCAD	1.04/1.75	160	7.00/5.15		
	Y-angular velocity	Positive peak alignment	2.21/2.10	160	7.55/6.25		
	X-displacement	Minimum DCAD*	0.76/1.38	160	2.80/2.60		
	Z-displacement	Minimum DCAD*	2.52/1.44	160	0.30/0.00		
T4	X-acceleration	Minimum DCAD	1.66/1.21	100	2.50/5.25	2.45	3.70
	Z-acceleration	None	0.87/1.02	100	0.00/0.00		
	Y-angular velocity	Positive peak alignment	1.51/1.06	160	4.90/5.80		
T8	X-acceleration	Minimum DCAD	1.24/0.91	100	4.20/5.45	2.25	3.40
	Z-acceleration	Minimum DCAD	1.03/0.85	100	0.00/1.05		
T12	X-acceleration	Minimum DCAD	1.40/1.00	100	8.50/9.80	3.12	4.65
	Z-acceleration	Minimum DCAD	1.05/0.68	100	0.00/1.05		
	Y-angular velocity	None	1.70/1.85	160	0.00/0.00		
Chest	Deflection	First peak	1.58/2.64	100	0.20/2.30	5.23	7.85
Pelvis	X-acceleration	Minimum DCAD	0.92/1.63	100	2.90/6.40	2.23	3.35
	Z-acceleration	Minimum DCAD	0.71/1.31	100	14.25/14.05		
	Y-rotation	First negative peak	3.37/3.04	160	3.70/6.50		
	X-displacement	None	2.37/2.27	160	0.00/0.00		
	Z-displacement	None	2.08/1.28	160	0.00/0.00		
	Y-angular velocity	Minimum DCAD	1.48/1.29	160	5.15/9.35		

TABLE CIII. SUMMARY OF BOUNDARY CONDITION BIOFIDELITY RANKING SCORE (BRS) CALCULATIONS FOR THE SAFER HBM V10 AND V11 IN THE UPRIGHT POSITION, INCLUDING THE METHOD OF ALIGNMENT FOR DUMMY CURVES (ADAPTED FROM [27]), TIME DURATION FOR THE BRS CALCULATION, ABSOLUTE VALUE OF DUMMY PHASE SHIFT (DPS) AND AVERAGE AND MAXIMUM OF ABSOLUTE VALUES OF PMHS SHIFT FOR SEAT REACTION LOADS AND BELT TENSIONS. DCAD = DUMMY CUMULATIVE ABSOLUTE DIFFERENCE.

Seat location	Seat reaction loads	Method of dummy curve alignment	BRS (v10/v11)	Time duration for BRS calculation (ms)	Absolute value of DPS (ms) (v10/v11)	Avg. of absolute value of PMHS shift (ms)	Max. of absolute value of PMHS shift (ms)
HR	Fx	Minimum DCAD	1.58/1.70	120	4.10/3.65	1.90	2.85
HR	Fz	First Peak	1.98/2.50	120	4.25/3.65	1.90	2.85
HR	My	Minimum DCAD	1.13/1.47	120	6.10/5.45	1.90	2.85
Seat back top	Fx	Minimum DCAD	2.20/2.05	100	0.00/0.85	1.88	2.70
Seat back middle	Fx	Minimum DCAD	3.06/2.79	100	3.45/6.10	2.27	3.40
Seat back bottom	Fx	Minimum DCAD	1.68/1.42	100	2.15/0.85	1.78	2.65
Shoulder belt	Tension	None	1.57/1.26	160	0.00/0.00	13.83	20.75
Lap belt	Tension	Minimum DCAD	0.71/0.70	160	8.75/10.45	4.15	6.20

TABLE CIV. SUMMARY OF AVERAGE BIOFIDELITY RANKING SYSTEM (BRS) SCORES FOR DIFFERENT BODY REGIONS IN COMPARISON WITH BRS SCORES FROM THE GHBMC M50 V6.0 FROM [28] AND THOR-50M IN PHYSICAL TESTS [27].

Body Region	SAFER HBM v10	SAFER HBM v11	GHBMC M50 V6.0 [28]	THOR ATD [27]
Head	1.48	1.51	1.82	2.31
Thoracic spine	1.38	1.23	1.81	1.33
Chest	1.58	2.64	2.67	0.84
Pelvis	1.82	1.80	2.07	2.48

XI. APPENDIX D – THOR UPRIGHT (25°) SIMULATION RESPONSES

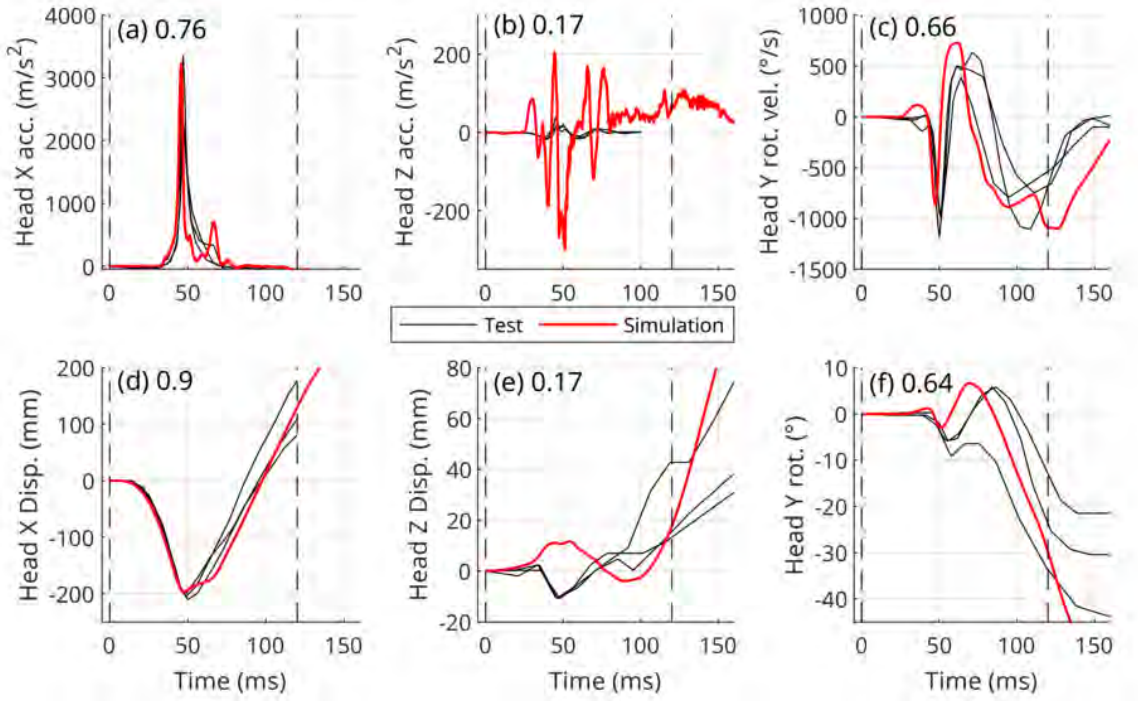

Fig. D1. THOR simulation head kinematics in the upright (25°) position compared with three tests from [27]. The number after the letter notation for each panel is the ISO score, and the time interval used for its calculation is indicated by the dashed lines. Acc. = Acceleration; Disp. = Displacement; Rot. = Rotation; Rot. Vel. = Rotational Velocity.

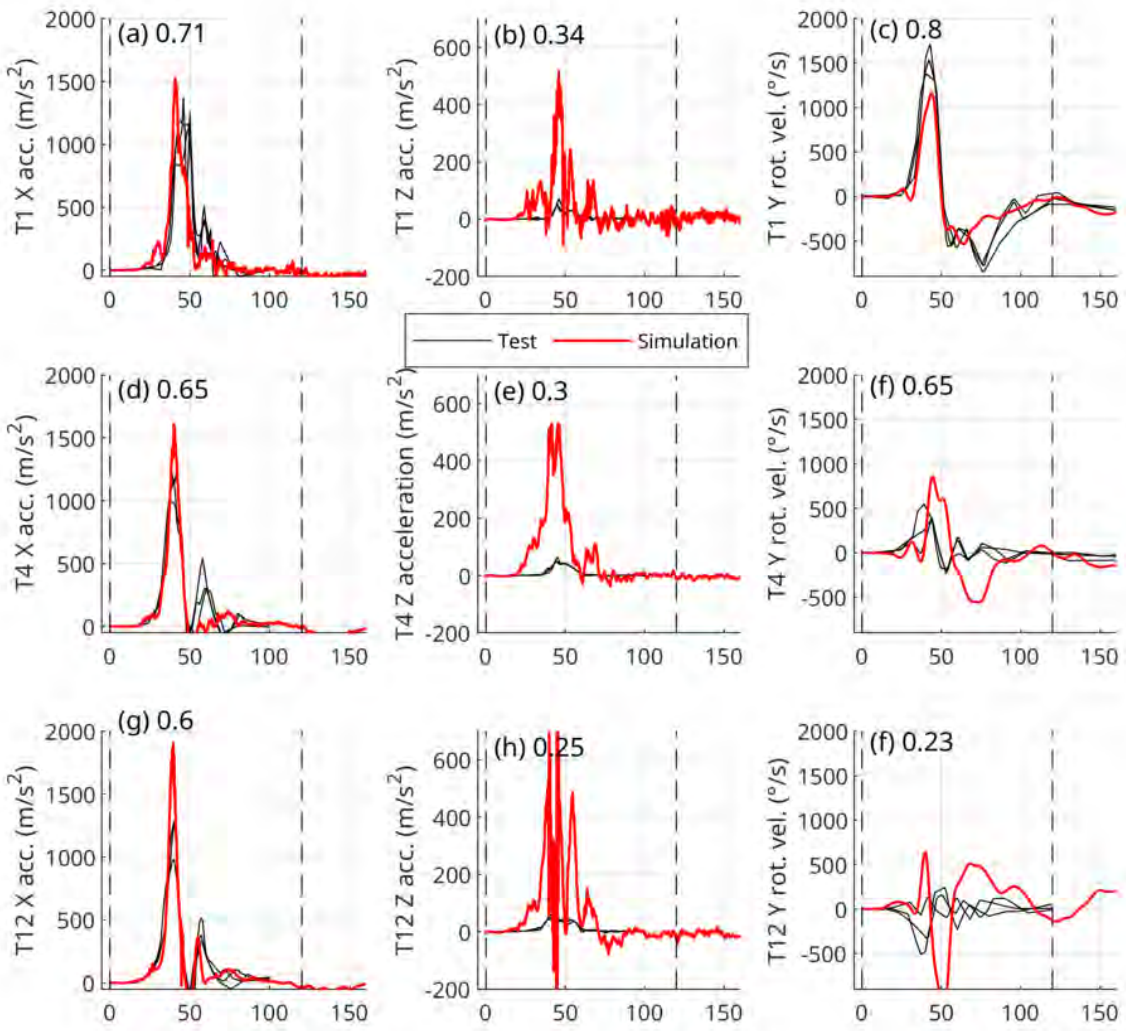

Fig. D2. THOR simulation torso kinematics in the upright (25°) position compared with three tests from [27]. The number after the letter notation for each panel is the ISO score, and the time interval used for its calculation is indicated by the dashed lines. Acc. = Acceleration; Disp. = Displacement; Rot. = Rotation; Rot. Vel. = Rotational Velocity.

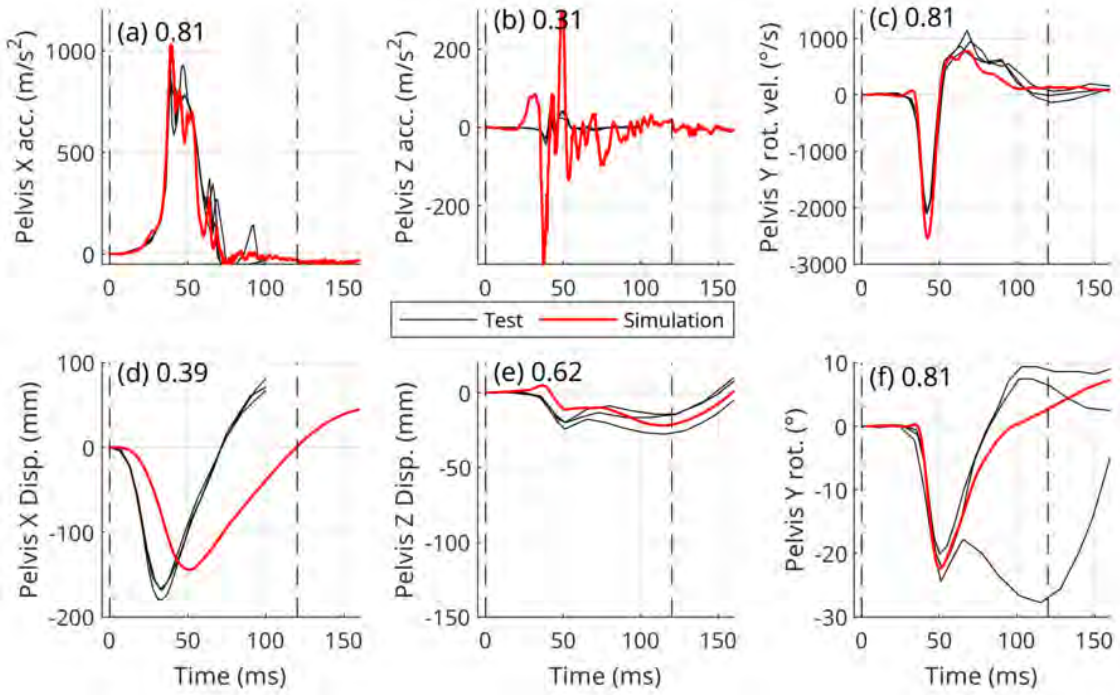

Fig. D3. THOR simulation pelvis kinematics in the upright (25°) position compared with three tests from [27]. The number after the letter notation for each panel is the ISO score, and the time interval used for its calculation is indicated by the dashed lines. Acc. = Acceleration; Disp. = Displacement; Rot. = Rotation; Rot. Vel. = Rotational Velocity.

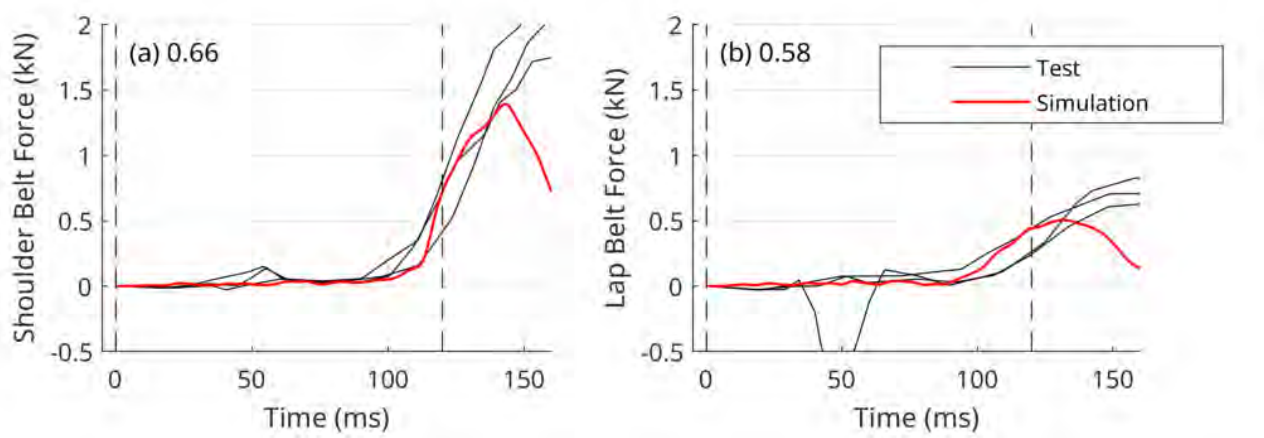

Fig. D4. THOR simulation seat belt forces in the upright (25°) position compared with three tests from [27]. The number after the letter notation for each panel is the ISO score, and the time interval used for its calculation is indicated by the dashed lines.

XII. APPENDIX E – THOR RECLINED (45°) SIMULATION RESPONSES

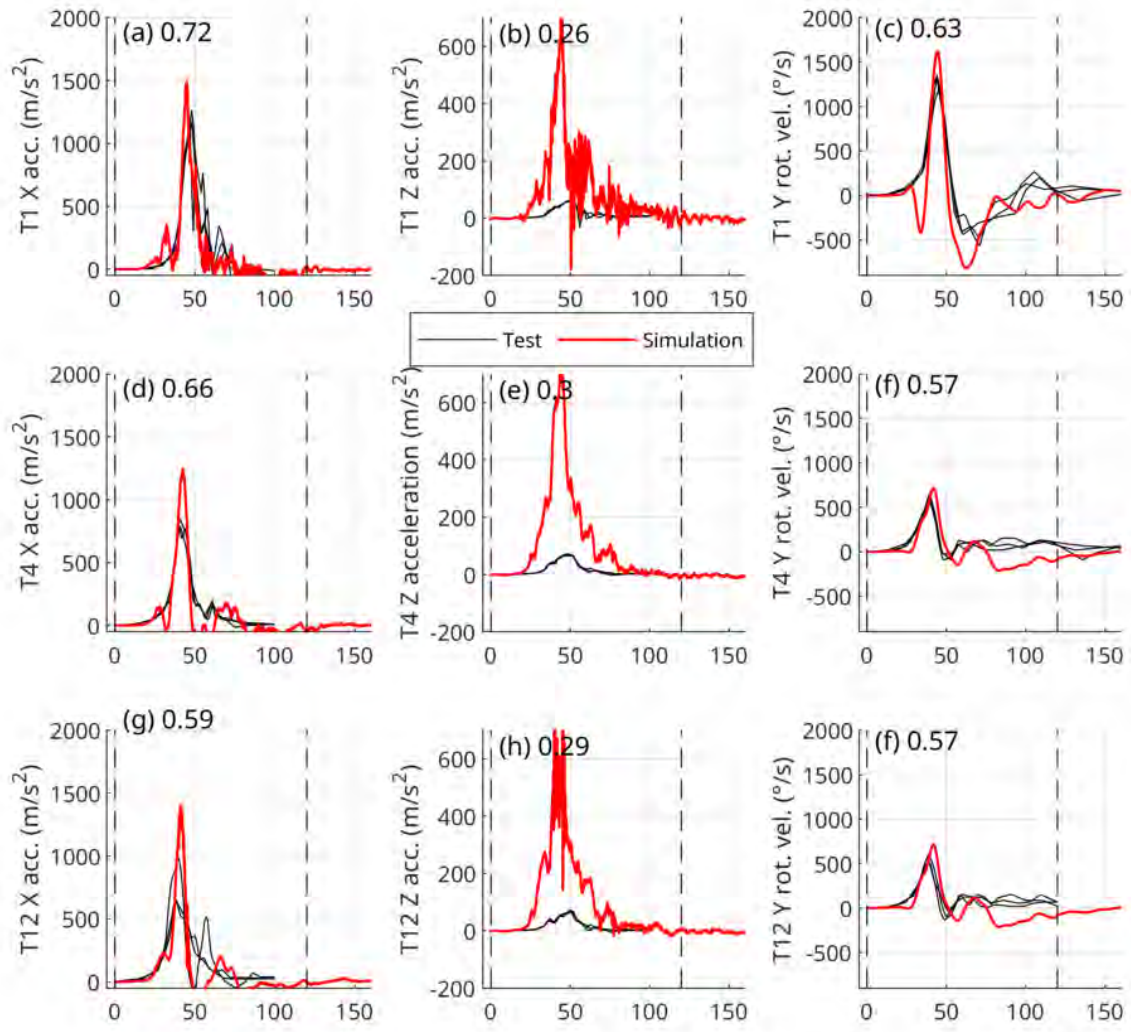

Fig. E1. THOR simulation torso kinematics in the reclined (45°) position compared with three tests from [27]. The number after the letter notation for each panel is the ISO score, and the time interval used for its calculation is indicated by the dashed lines. Acc. = Acceleration; Disp. = Displacement; Rot. = Rotation; Rot. Vel. = Rotational Velocity.

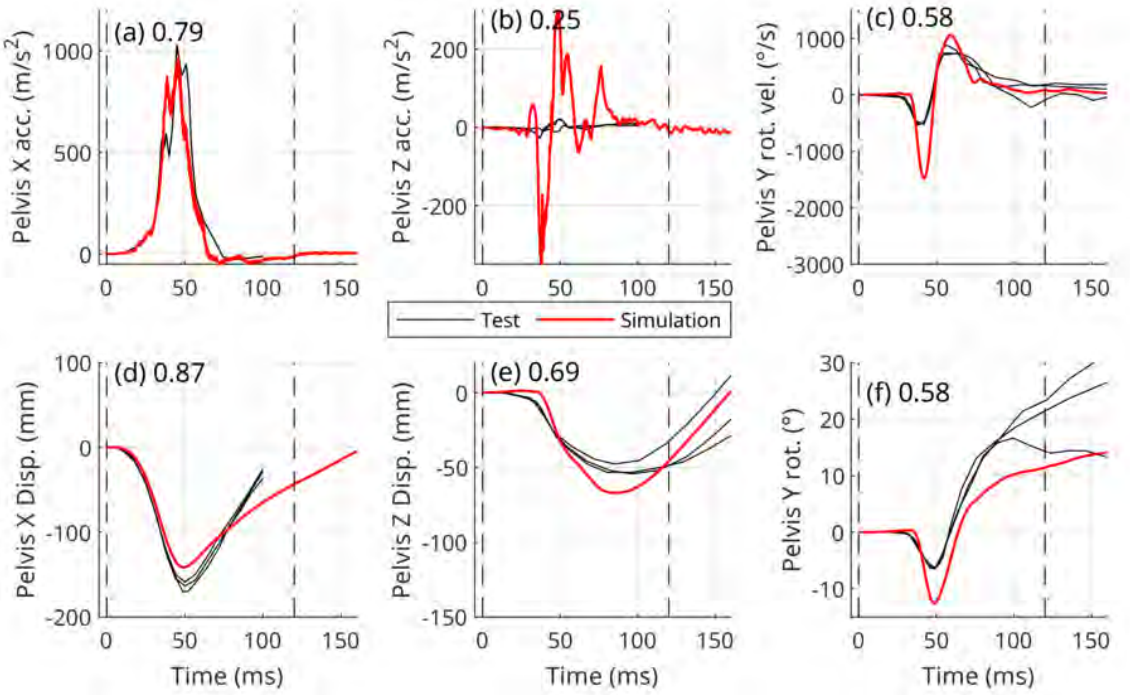

Fig. E2. THOR simulation pelvis kinematics in the reclined (45°) position compared with three tests from [27]. The number after the letter notation for each panel is the ISO score, and the time interval used for its calculation is indicated by the dashed lines. Acc. = Acceleration; Disp. = Displacement; Rot. = Rotation; Rot. Vel. = Rotational Velocity.

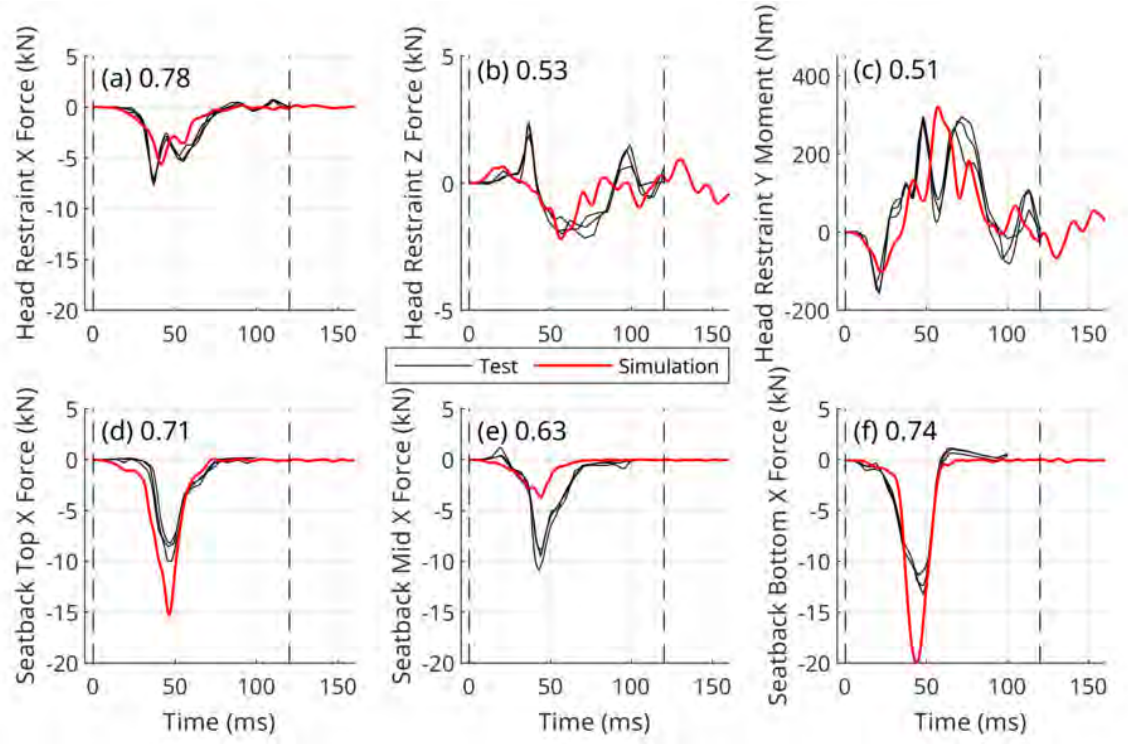

Fig. E3. THOR simulation boundary conditions in the reclined (45°) position compared with three tests from [27]. The number after the letter notation for each panel is the ISO score, and the time interval used for its calculation is indicated by the dashed lines.

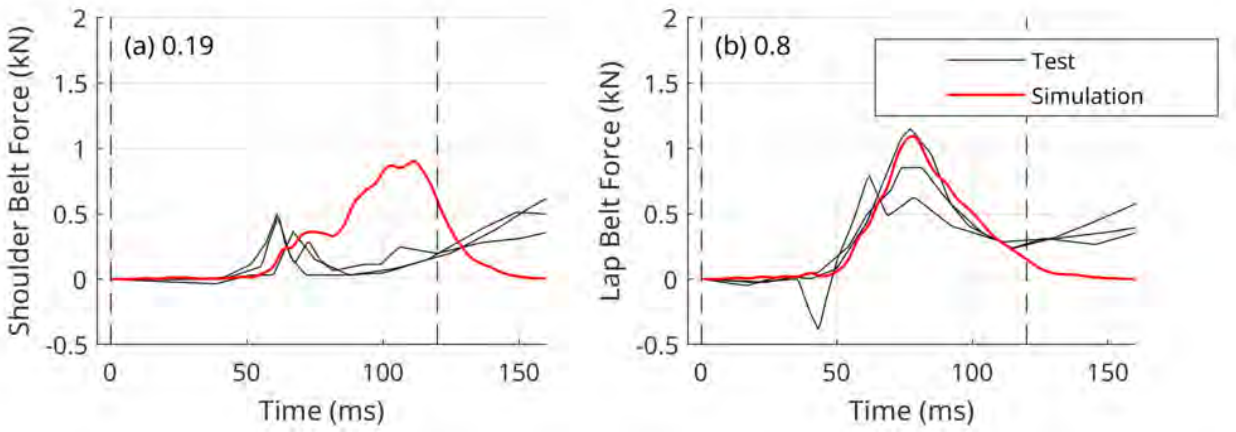

Fig. E4. THOR simulation seat belt forces in the reclined (45°) position compared with three tests from [27]. The number after the letter notation for each panel is the ISO score, and the time interval used for its calculation is indicated by the dashed lines.

XIII. APPENDIX F – HBM UPRIGHT (25°) SIMULATION RESPONSES

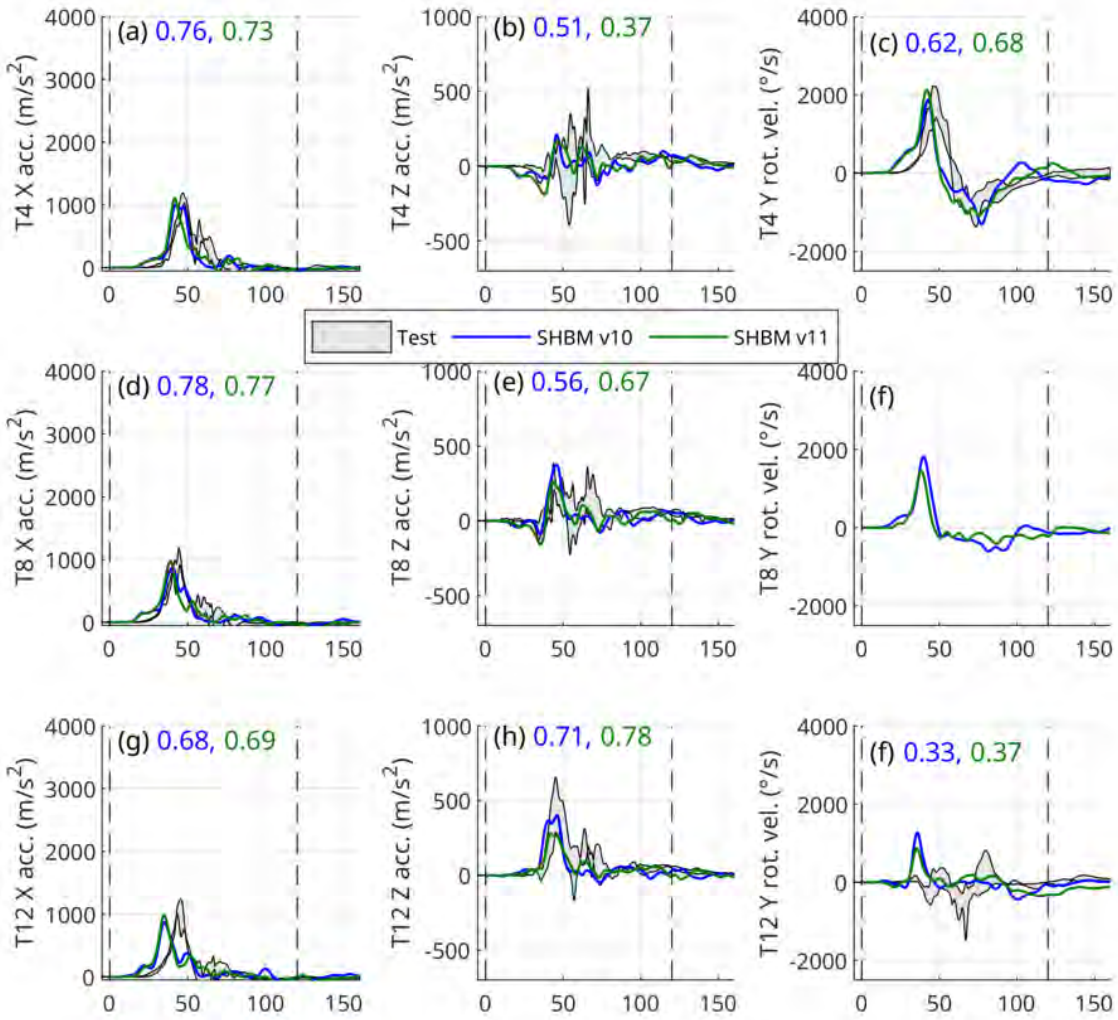

Fig. F1. HBM T4-T12 kinematics in the upright (25°) position in comparison with PMHS data [26]. The number after the letter notation for each panel is the ISO score, and the time interval used for its calculation is indicated by the dashed lines. Acc. = Acceleration; Disp. = Displacement; Rot. = Rotation; Rot. Vel. = Rotational Velocity.

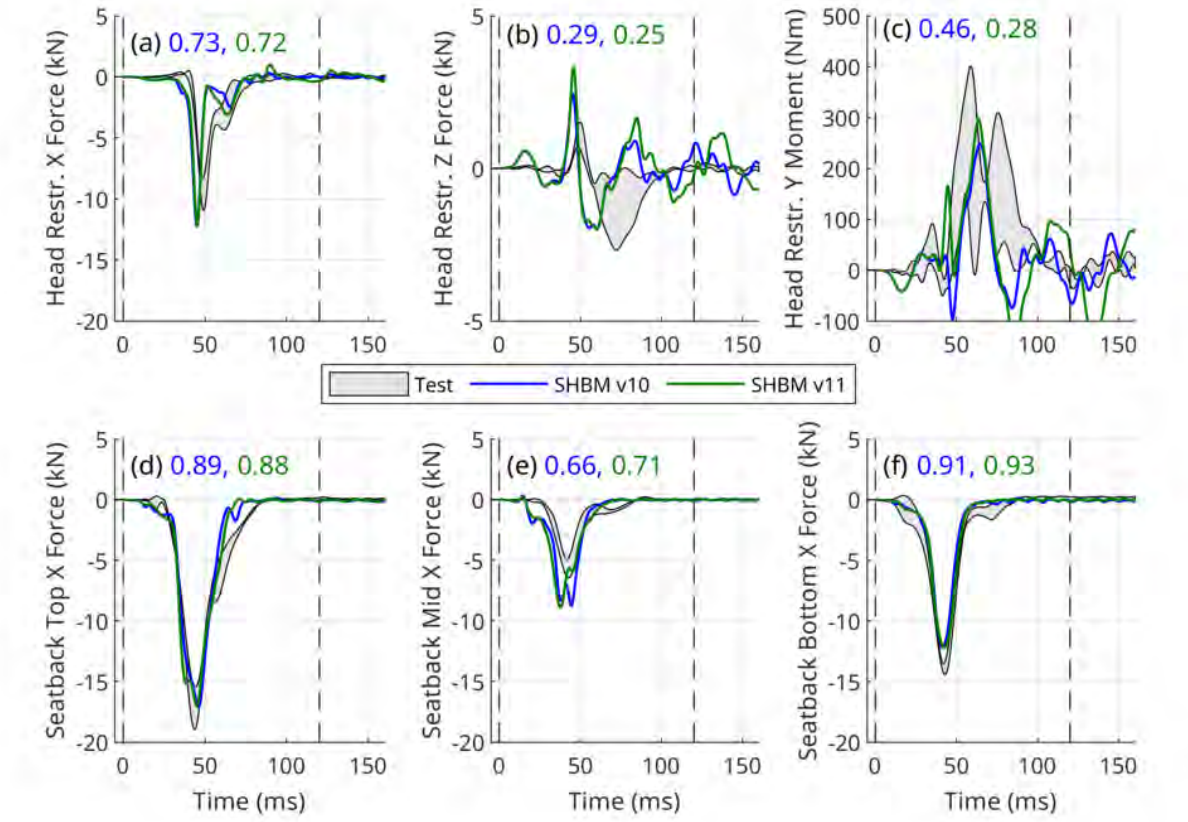

Fig. F2. HBM head restraint and seat back boundary conditions in the upright (25°) position in comparison with PMHS data [26]. The number after the letter notation for each panel is the ISO score, and the time interval used for its calculation is indicated by the dashed lines.

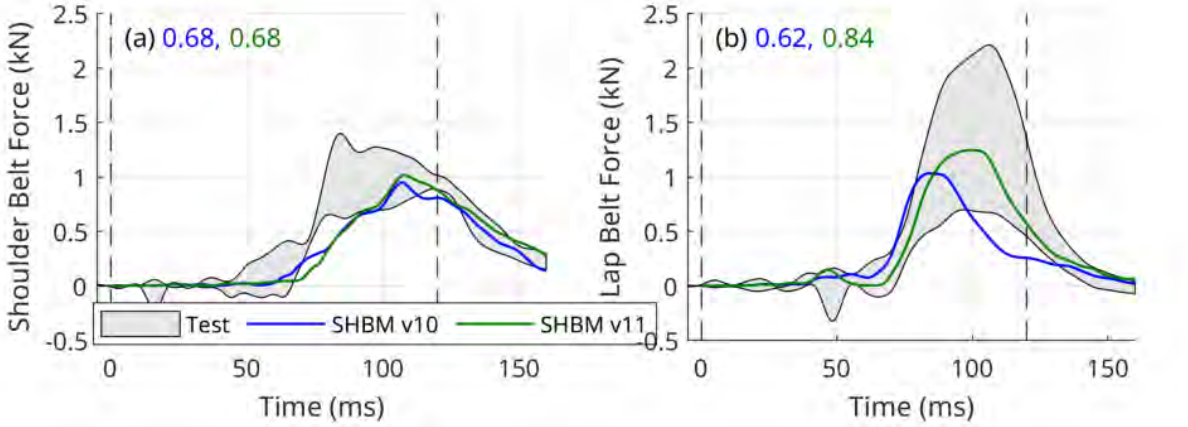

Fig. F3. HBM seat belt forces in the upright (25°) position in comparison with PMHS data [26]. The number after the letter notation for each panel is the ISO score, and the time interval used for its calculation is indicated by the dashed lines.

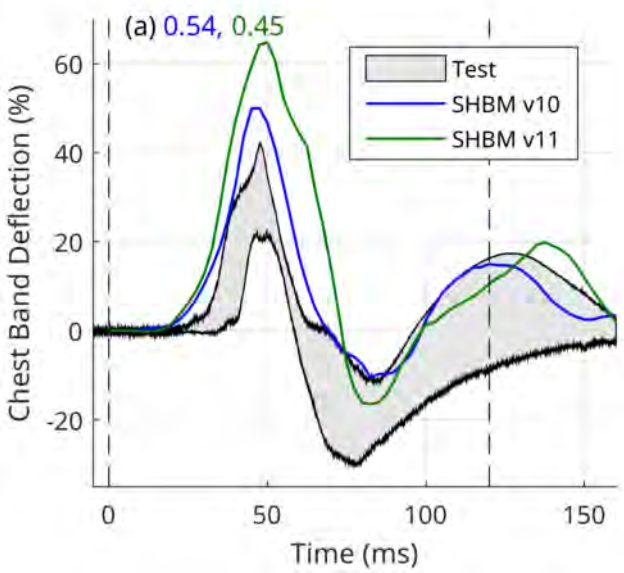

Fig. F4. HBM half-width normalized chest band deflections in the upright (25°) position in comparison with PMHS data [26]. The number after the letter notation for each panel is the ISO score, and the time interval used for its calculation is indicated by the dashed lines.

XIV. APPENDIX G – HBM RECLINED (45°) SIMULATION RESPONSES

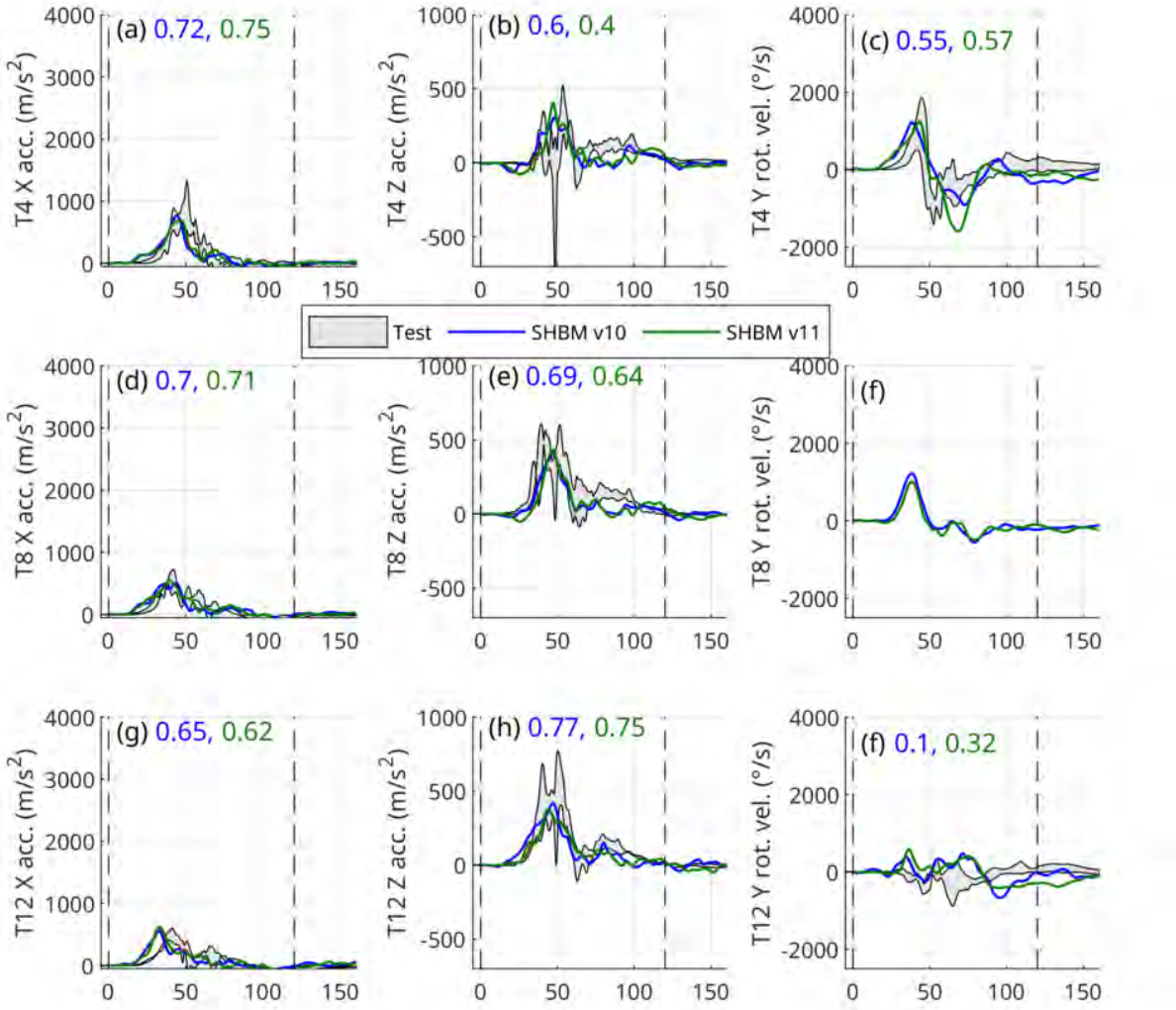

Fig. G1. HBM T4-T12 kinematics in the reclined (45°) position in comparison with PMHS data [26]. The number after the letter notation for each panel is the ISO score, and the time interval used for its calculation is indicated by the dashed lines. The vertical dashed lines indicate the time interval used for the ISO score calculation. Acc. = Acceleration; Disp. = Displacement; Rot. = Rotation; Rot. Vel. = Rotational Velocity.

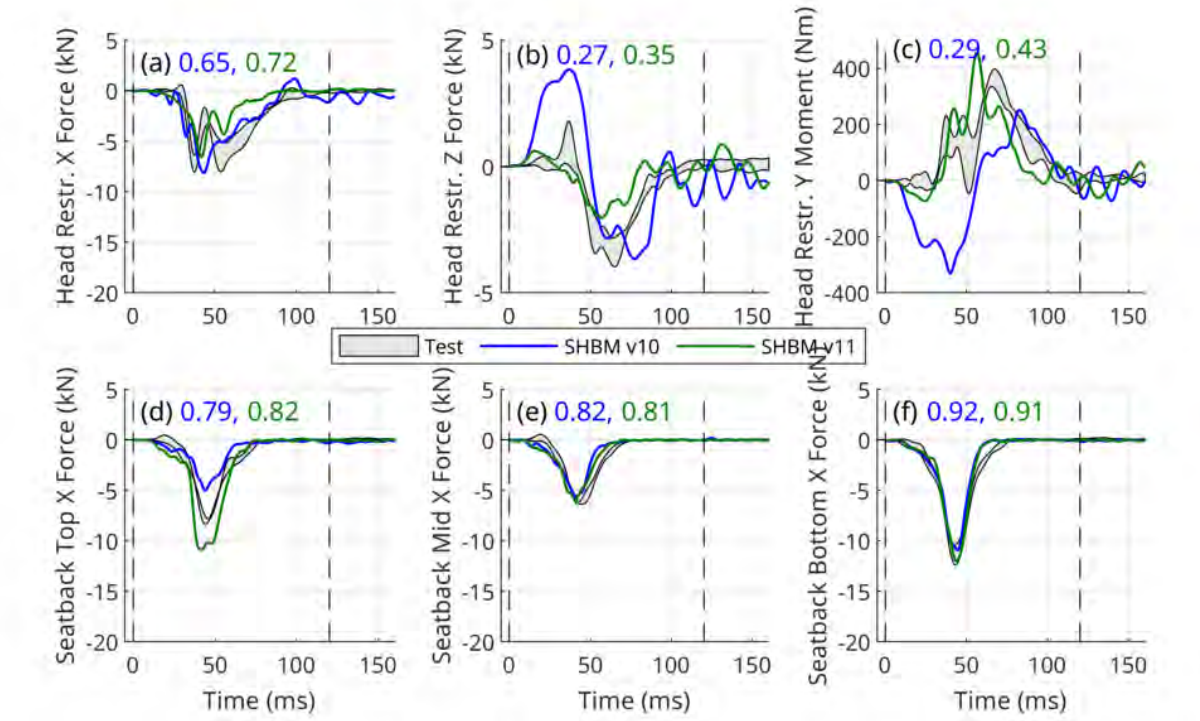

Fig. G2. HBM head restraint and seat back boundary conditions in the reclined (45°) position in comparison with PMHS data [26]. The number after the letter notation for each panel is the ISO score, and the time interval used for its calculation is indicated by the dashed lines.

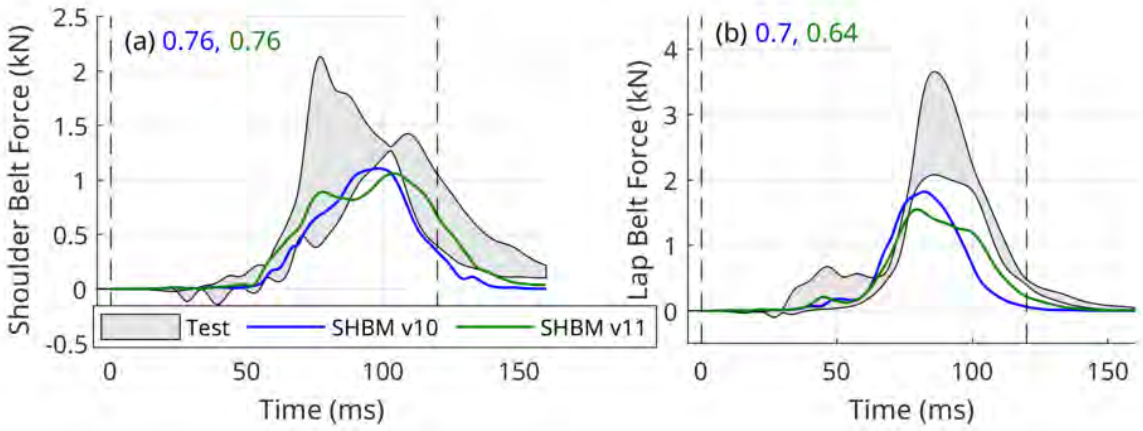

Fig. G3. HBM seat belt forces in the reclined (45°) position in comparison with PMHS data [26]. The number after the letter notation for each panel is the ISO score, and the time interval used for its calculation is indicated by the dashed lines.

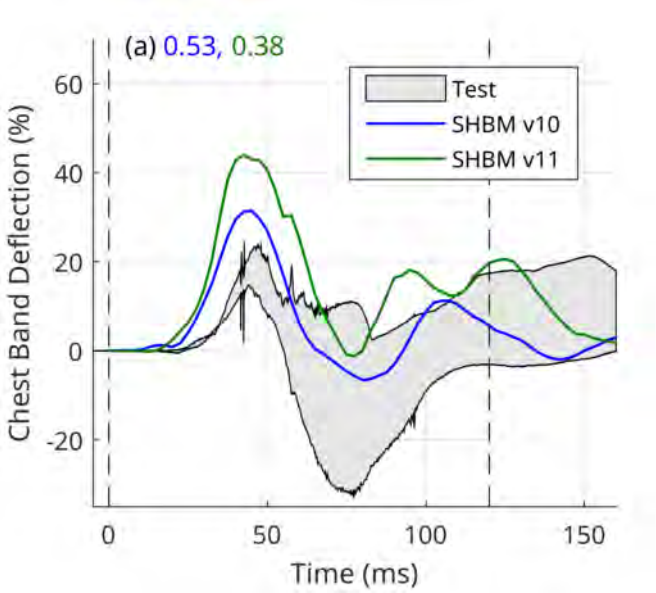

Fig. G4. HBM half-width normalized chest band deflections in the reclined (45°) position in comparison with PMHS data [26]. The number after the letter notation for each panel is the ISO score, and the time interval used for its calculation is indicated by the dashed lines.